TECHNICAL REPORT STANDARD TITLE PAGE

1. Report No.	2. Government Accession No.	3. Recipient's Catalog No.
FHWA/TX-86/47+386-1		

4. Title and Subtitle	5. Report Date
EXPERIMENTAL INVESTIGATION OF TRUCK TIRE INFLATION PRESSURE ON PAVEMENT-TIRE CONTACT AREA AND PRESSURE DISTRIBUTION	August 1985
	6. Performing Organization Code

7. Author(s)	8. Performing Organization Report No.
Kurt M. Marshek, W. Ronald Hudson, Richard B. Connell, Hsien H. Chen, and Chhote L. Saraf	Research Report 386-1

9. Performing Organization Name and Address	10. Work Unit No.
Center for Transportation Research The University of Texas at Austin Austin, Texas 78712-1075	11. Contract or Grant No. Research Study 3-8-84-386
	13. Type of Report and Period Covered Interim
12. Sponsoring Agency Name and Address Texas State Department of Highways and Public Transportation; Transportation Planning Division P. O. Box 5051 Austin, Texas 78763	14. Sponsoring Agency Code

15. Supplementary Notes

Study conducted in cooperation with the U. S. Department of Transportation, Federal Highway Administration. Research Study Title: "The Magnitude of Tire Pressures on Texas Highways and the Effect of Tire Pressures on Flexible and Rigid Pavements"

16. Abstract

This report contains the results of an experimental investigation into the gross contact areas and contact pressure distributions produced by statically loaded truck tires. The gross contact areas are determined using an automatic imaging system that computes the contact area from a digitized data base obtained from an inked tire print. Contact pressure distributions produced by statically loaded tires are determined using a pressure sensitive film technique.

17. Key Words	18. Distribution Statement
tire pressures, truck tires, contact area, contact pressure distribution, axle loads, pavements	No restrictions. This document is available to the public through the National Technical Information Service, Springfield, Virginia 22161.

19. Security Classif. (of this report)	20. Security Classif. (of this page)	21. No. of Pages	22. Price
Unclassified	Unclassified	62	

Form DOT F 1700.7 (8-69)

EXPERIMENTAL INVESTIGATION OF TRUCK TIRE INFLATION PRESSURE ON PAVEMENT-TIRE CONTACT AREA AND PRESSURE DISTRIBUTION

by
Kurt M. Marshek
W. Ronald Hudson
Richard B. Connell
Hsien H. Chen
Chhote L. Saraf

Research Report Number 386-1

The Magnitude of Tire Pressures on Texas Highways and the Effect of Tire Pressures on Flexible and Rigid Pavements
Research Project 3-8-84-386

conducted for

Texas State Department of Highways and Public Transportation

in cooperation with the
U. S. Department of Transportation
Federal Highway Administration

by the

Center for Transportation Research
The University of Texas at Austin

August 1985

The contents of this report reflect the views of the authors, who are responsible for the facts and the accuracy of the data presented herein. The contents do not necessarily reflect the official views or policies of the Federal Highway Administration. This report does not constitute a standard, specification, or regulation.

PREFACE

This is the first of two reports which describe work done on Project 386, " The Magnitude of Tire Pressures on Texas Highways and the Effect of Tire Pressures on Flexible and Rigid Pavements." The study is being conducted at the Center for Transportation Research (CTR), The University of Texas at Austin, as part of a cooperative research program sponsored by the Texas State Department of Highways and Public Transportation and the Federal Highway Administration.

Many people have contributed their help toward the completion of this report. Thanks are extended to Dr. B. Frank McCullough for his help and guidance and to all the CTR personnel, especially Lyn Gabbert, Raul Longoria, Monica Gonzalez, Loretta McFadden, Art Frakes, John Ermis, Donna Williams, and Kitty Collins. Invaluable comments were provided by Robert L. Mikulin, Jerome F. Daleiden, and James L. Brown, all from the Texas State Department of Highways and Public Transportation, and by Edward V. Kristaponis, from the Federal Highway Administration.

Some of the material presented in this report was collected and reported on by the following students as part of several student design projects at the University of Texas at Austin: Dennis Hilton, Leonard L. Leinweber, Curtis Prothe, John Salazar, John Bishop, Daniel Lodge, Will Nelson, John Trelford, Melford S. Carter, Scott R. Corbett, Mark Emerson, Youssef Fakhreddine, Keith W. Heugatter, John A. Varela, David Calvillo-Villareal, Luis Javier Gonzalez, and Raul G. Longoria. Dr. Leonardt F. Kreisle was the director of the student design course under which the design teams were organized. We acknowledge their contributions and greatly appreciate their efforts to make this a successful project.

Kurt M. Marshek
W. Ronald Hudson
Richard B. Connell

August 1985

LIST OF REPORTS

Report No. 386-1, "Experimental Investigation of Truck Tire Inflation Pressure on Pavement-Tire Contact Area and Pressure Distribution," by Kurt M. Marshek, W. Ronald Hudson, Richard B. Connell, Hsien H. Chen, and Chhote L. Saraf, presents data on the effect of truck tire pressure and load on contact area, and pressure distribution. August 1985.

Report No. 386-2F, "Effect of Truck Tire Inflation Pressure and Axle Load on Pavement Performance," by Kurt M. Marshek, W. Ronald Hudson, Hsien H. Chen, Chhote L. Saraf, and Richard B. Connell, presents an analytical evaluation of the effect of truck tire inflation pressure on pavement performance. August 1985.

ABSTRACT

This report contains the results of an experimental investigation into the gross contact areas and contact pressure distributions produced by statically loaded truck tires. The gross contact areas are determined using an automatic imaging system that computes the contact area from a digitized data base obtained from an inked tire print. Contact pressure distributions produced by statically loaded tires are determined using a pressure sensitive film technique.

KEY WORDS: tire pressures, truck tires, contact area, contact pressure distribution, axle loads, pavements

SUMMARY

This report presents the results of an experimental study (a) to determine the effect of inflation pressure and axle load on gross contact area and (b) to determine pressure distributions beneath statically loaded truck tires using a pressure sensitive film. A load frame fitted with a hydraulic ram was used to statically load the truck tires tested. An inked tire print was read by an automatic imaging system to determine the gross contact area of the tires. The use of pressure sensitive film allowed the entire pressure distribution to be captured. The data from the pressure distribution stored using an automated print reading system.

The results of the contact area study show that (a) increasing the tire inflation pressure reduces the gross contact area of statically loaded truck tires and (b) increasing the axle load produces an increase in gross contact area.

The results of the contact pressure distribution study show that the treaded tire produced the highest pressures in the tire shoulder region for the cases studied. With higher inflation pressures the peak contact pressures moved from the tire shoulder region towards the tire centerline. The results also show that heavy axle loads produced regions of high pressure in the tire shoulder region. Experiments conducted on a bald tire show similiar trends. However, the overall pressure distribution was more continuous due to the lack of treads.

IMPLEMENTATION STATEMENT

The work carried out under this project provides tire contact areas and pavement-tire pressure distributions for truck tires at several inflation pressures and axle loads. The tire contact areas and pressure distributions are available for use in evaluating the effect of truck tire inflation pressure and axle load on the structural adequacy and capacity of flexible and rigid pavements. Such information and evaluations could lead to changes in methods employed for current highway design to improve the structural capacity of pavements and/or overlay design, or produce recommendations for legislation to regulate truck tire inflation pressure and axle load.

TABLE OF CONTENTS

CHAPTER 1. INTRODUCTION

One of the major costs incurred by the Texas State Department of Highways and Public Transportation is for maintaining public roads in a serviceable condition. A variety of factors are known to contribute to pavement damage in Texas. These include climate, traffic density, and the loads from car and truck tires.

Historically, the subject of contact pressure distribution between a tire and a pavement has received little attention for several reasons: simplifying assumptions made in past road design work made knowledge of the actual pressure distribution unnecessary, and measurements of the contact pressure at all locations (points) in the tire footprint were difficult to make. The actual contact pressure distribution between the tire and the pavement will undoubtedly play a larger role in highway design once its role in pavement damage is better understood.

BACKGROUND

The assumption is commonly made that the contact pressure acts on an area that is circular in shape and that the contact pressure is uniform and equal in magnitude to the tire inflation pressure (Ref 1). This assumption simplifies considerably the theoretical relationships used by highway engineers in design work.

In order to determine the size and shape of the net contact area, Flugrad and Miller (Ref 2) modeled the tire as a modified standing torus in their finite element analysis and predicted an elliptical contact area. Another study by Mack et al (Ref 3) also modeled the tire as a standing torus, again predicting an elliptical contact area.

The actual shape of the contact area of a pneumatic tire deviates from an ellipse primarily due to the presence of treads and reinforcing cords in the tire carcass. Furthermore, the cord angle affects the contact area shape, with radial tires producing an almost rectangular footprint and bias ply tires producing an approximate ellipse.

One of the most common methods for experimentally determining the size and shape of the net contact area is to ink the tire to be tested before applying the load. The inked areas on the prints can then be cut out and weighed. The weight and total area of the inked portions (net contact area) are directly proportional to that of the entire print, whose weight and total area are known. O'Neil (Ref 4) experimentally determined the net contact area of a statically loaded tire by coating the tire with oil, loading the tire on paper, and then allowing graphite particles to stick to the oily parts of the paper. Tracing of the image obtained then gave the desired net contact area.

The contact pressure distribution beneath statically loaded truck tires is difficult to determine analytically; the non-uniform geometry of the tire, and the presence of treads and reinforcing cords in the tire carcass, complicates the problem beyond an exact analytical solution. The use of sophisticated theoretical relationships in determining the contact pressure distribution is questionable, however, since the answers obtained from the theoretical relationships do not agree well with data from tire experiments.

The pressure distribution can also be determined by using computer analysis programs. One advantage gained using computer analyses is that more realistic tire models can be used, due to the increased computational capabilities. Mack, et al (Ref 3) applied a finite element analysis to a tire (modeled as a thin-walled pressurized torus) under a normal load in order to determine stresses in the tire. Tielking (Ref 5) improved the torus model by adding additional mass to the shoulder region of the

tire; the resulting pressure distribution showed a peak pressure (approximately twice the inflation pressure) occuring roughly mid-way between the tire centerline and shoulder. There are other studies that attempt to analytically predict the pressure distribution beneath a pneumatic tire; however, the complexity of the problem has prevented an exact solution from being obtained.

The most common method for experimentally determining the contact pressure distribution is through the use of pressure transducers. For statically loaded tires, O'Neal (Ref 4) used a nylon pin and proving ring assembly to determine the normal and tangential pressure distributions exerted by the tire. Diaphram strain gages are also commonly used in this application (Ref 9).

A study by Marshek, et al in progress at The University of Texas at Austin uses a digitizing camera and data acquisition system to determine the contact pressure distribution and the net contact area from pressure sensitive film prints of statically loaded truck tires. The camera digitizes the print and then, using this data base, (1) displays the pressure distribution and (2) calculates the net contact area by summing the pixels (picture elements on the video monitor) on the digitized image.

The measurement of the dynamic load produced by a tire usually involves mounting the transducers in a flat bed or rotating drum. Lippmann and Oblizajek (Ref 6) used specially designed microtransducers mounted in a ground steel bed to record three components (normal, radial, and tangential) of the pressure distribution under freely rolling tires. Shimada et al (Ref 7) conducted a study using piezo-electric sensors mounted in a rotating drum to measure various contact forces at high speeds.

OBJECTIVES

The objectives of this study were to determine (1) the gross contact area for a number of statically loaded truck tires using a variety of tire inflation pressure and axle load combinations and (2) the contact pressure distribution for a bald and treaded tire using a pressure sensitive film technique. The data obtained will indicate what effect the tread pattern, tire inflation pressure, and axle load have on the resulting tire-pavement contact area and contact pressure distributions.

SCOPE AND ORGANIZATION

Chapter 1 serves as an introduction to this report.

Chapter 2 describes the experimental apparatus and procedure used to determine the gross contact area for eight truck tires under static loading conditions. The effects of tire inflation pressure and axle load on the gross contact area are discussed. Also, results are presented and conclusions drawn.

In Chapter 3, the experimental apparatus and test procedure used to determine the contact pressure distribution for various tire inflation pressures and axle loads are described. Experimental results are presented and discussed and conclusions are drawn.

Chapter 4 presents a summary of the conclusions and recommendations made throughout the report.

CHAPTER 2. EXPERIMENTAL INVESTIGATION OF GROSS CONTACT AREA

This chapter discusses the experimental apparatus and experimental procedure used to obtain (using an inked print and digitizing camera system) the gross contact area from eight statically loaded tires. The principal objective is to show the effect of tread pattern, tire inflation pressure, and axle load on the resulting gross contact area for statically loaded tires.

EXPERIMENTAL APPARATUS

The experimental apparatus used in this study consisted of the following components: eight truck tires, a load frame for statically loading tires, paper and printers' ink for capturing the tire-pavement contact areas, and a Grinnell Imaging System for measuring the contact areas.

Tires

Eight truck tires were used to determine how the tire construction (bias ply or radial) and dimensions affected the size and shape of the gross contact area. The following tires were used in this study: a Goodyear 10-20, a Uniroyal 10-20, a Goodyear 11-22.5, a Bridgestone 11-22.5, a Bridgestone 11-24.5, a Goodyear 10R-20, a Goodyear 11R-22.5, and a Bridgestone 16.5R-22.5, where an R appended to the first digit of the tire number indicates a radial tire. Table 2.1 gives a complete description of the tires used in this study.

Load Frame

The truck tires studied were statically loaded with the load frame shown in Figure 2.1. The frame was designed so that a hydraulic ram mounted above the tire assembly could deliver a load to the tire through the shaft running through the tire hub. This design allowed the tire to be loaded to simulate actual use, in contrast to loading the tire, for example, by placing weights on the top of the tire.

Grinnell Imaging System

The gross contact areas of the inked tire prints were measured with the Advanced Graphics Laboratory's Grinnell Image Processing System. The Grinnell System manipulates and stores a high resolution video picture which is 512 pixels (picture elements) wide and 512 tall. The black-and-white digitizing camera can differentiate between 256 levels of light intensity for each pixel in the video picture. Data obtained from the camera was stored on disc by the data acquisition system.

EXPERIMENTAL PROCEDURE

The experimental procedure used to determine the gross contact area of the statically loaded truck tires consisted of the following two parts: (1) obtaining an inked tire print for each test conducted and (2) measuring the gross contact area for each print, using the Grinnell System.

The tire to be tested was mounted on the load frame described earlier and was cleaned on the anticipated contact surface of the tire. The tire was then inked and statically loaded onto a piece of paper

TABLE 2.1: DIMENSIONS OF TIRES TESTED

	Goodyear 10x20 Super Hi-Miler	Goodyear 11x22.5 Super Hi-Miler	Goodyear 10Rx20 G186 Unisteel	Goodyear 11Rx22.5 Super Hi-Miler	Uniroyal 10x20 Fleetmaster Triple Tread	Bridgestone 11x22.5 Super L-Miler	Bridgestone 11x24.5 Super L-Miler	Bridgestone 16.5Rx22.5 V-steel Mix 747
Weight of the tire and wheel assembly	182	176.5	219.5	190	200.5	199	194	333.5
Elevation of center tread over sidewall	1/2	5/8	3/8	1/4	1/2	1/2	1/2	3/8
Wheelwidth	8	8	8	7 1/2	6	8	8	14 1/2
Wheel/Bead Diameter	20	22 1/2	20	22 1/2	20	22 1/2	24 1/2	22 1/4
Sidewall width	11 1/4	10 7/8	10 3/4	10 1/4	11	11 1/4	11	16 3/4
Outside Diameter	41 5/8	41 1/4	41 9/16	41 3/16	41 1/4	42	43 5/8	44 1/4
Sidewall plies	6 nylon	6 nylon	1 steel	1 steel	6 nylon	6 nylon	6 nylon	1 steel
Tread plies	8 nylon	8 nylon	5 steel	5 steel	8 nylon	8 nylon	8 nylon	5 steel
Rated inflation pressure	85	85	105	105	85	85	85	110
Rated load (single)	5430	5430	6040	6040	5430	5430	5780	10210

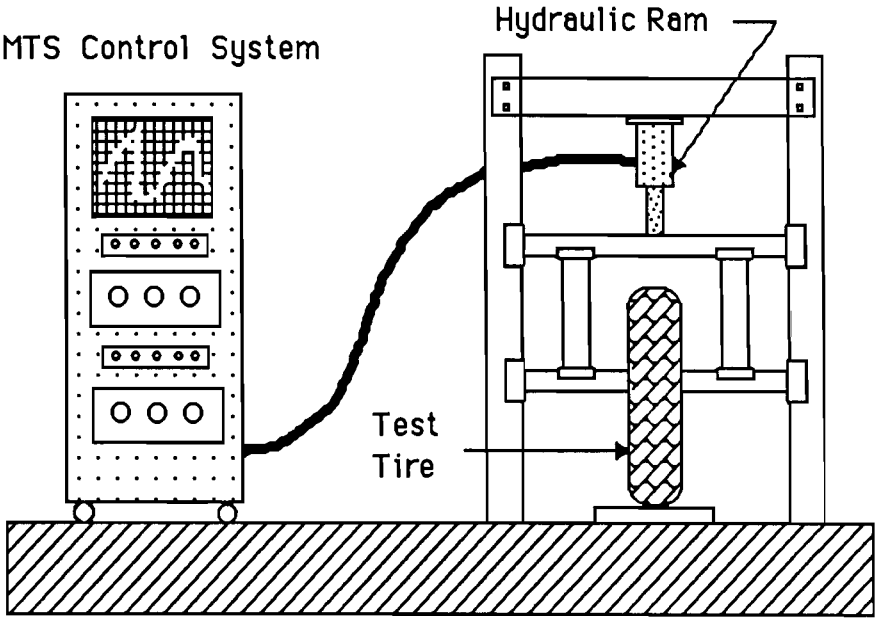
MTS Control System
Hydraulic Ram
Test
Tire

(taped to a smooth, flat, steel plate) using the MTS hydraulic control system. The load on the tire was then released and the inked tire print set aside to dry.

To measure the gross contact area of the tire footprint, the inked print was taped to a vertical screen in front of the digitizing camera. The camera was then focused on the print and the data stored by the data acquisition system. A more complete description of the Grinnell Imaging System and the operating procedure appear in Ref 8.

PRESENTATION AND DISCUSSION OF RESULTS

The presentation and discussion of results is divided into two sections, the first discussing inflation pressure effects on gross contact area, and the second discussing axle load effects. The results of the gross contact area study are given in the form of plots showing the effect of tire inflation pressure and axle load on contact area for the tires tested.

Inflation Pressure

Figure 2.2 shows the effect of tire inflation pressure on the gross contact area for the Goodyear 11R-22.5, Bridgestone 11-22.5, Goodyear 11-22.5, and the Bridgestone 16.5R-22.5 tires each at their rated axle load -- see Table 2.1. The plotted data confirms the results of other investigations, which also show a reduction in gross contact area for an increase in tire inflation pressure (Refs 1,10). The plot shows that the radial tire develops a smaller contact area than the bias ply tires (for a given tire size and inflation pressure) over the range of inflation pressures studied. The plot also shows that the16.5R-22.5 tire undergoes larger changes in contact area, with changing inflation pressure, than do the 11-22.5 tires. In general, for an increase in tire inflation pressure of about 50%, there was a corresponding decrease in gross contact area of approximately 8% to 20% for the tires shown in Fig. 2.2 each at their rated axle load.

Figures 2.3 and 2.4 show that the trend of decreasing gross contact area with increasing tire inflation pressure persists for the Goodyear 11R-22.5 and Goodyear 11-22.5 tires, through the range of inflation pressures studied.

Axle Load

Figure 2.5 shows the effect of axle load on the gross contact area for the Goodyear 11R-22.5, Bridgestone 11-24.5, Uniroyal 10-20, and Bridgestone 16.5R-22.5 truck tires each at their rated inflation pressure -- see Table 2.1. The plot confirms the anticipated result that an increase in axle load produces an increase in gross contact area. For an increase in the axle load of 50%, there was a corresponding increase in gross contact area of approximately 30% to 35%. Figures 2.6 and 2.7 show that this trend persists for the Goodyear 10-20 and Goodyear 11R-22.5 tires in the range of tire inflation pressures studied. The plots show that there is close to a linear relationship between gross contact area and axle load, and that the contact area growth rates for bias ply tires and radial tires with increasing axle load are approximately equal.

CONCLUSIONS

The results of the gross contact area study based on the Grinnell Imaging System can be summarized as follows:

1. An increased tire inflation pressure produced a smaller gross contact area. For an increase in tire inflation pressure of about 50%, there was a corresponding decrease in gross contact area of approximately 8% to 20%.

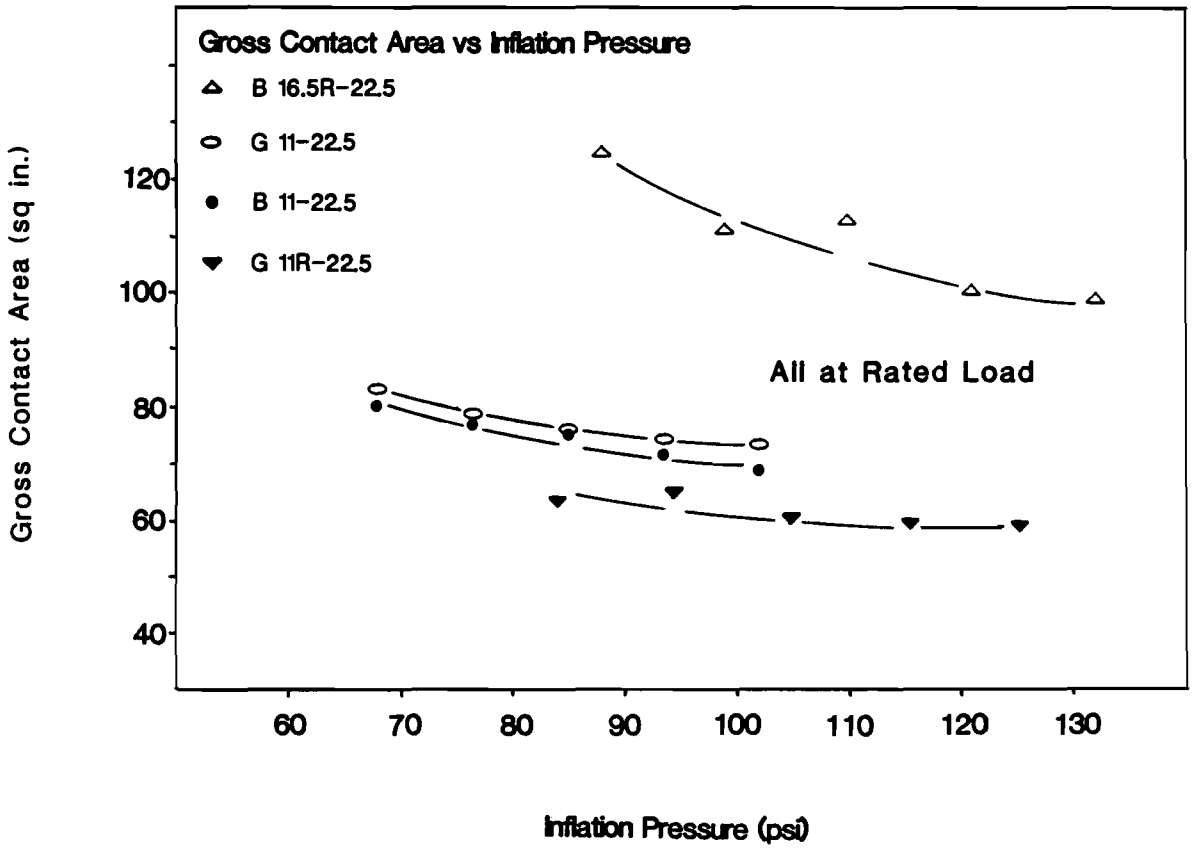

Fig. 2.2: Effect of Inflation Pressure on Gross Contact Area

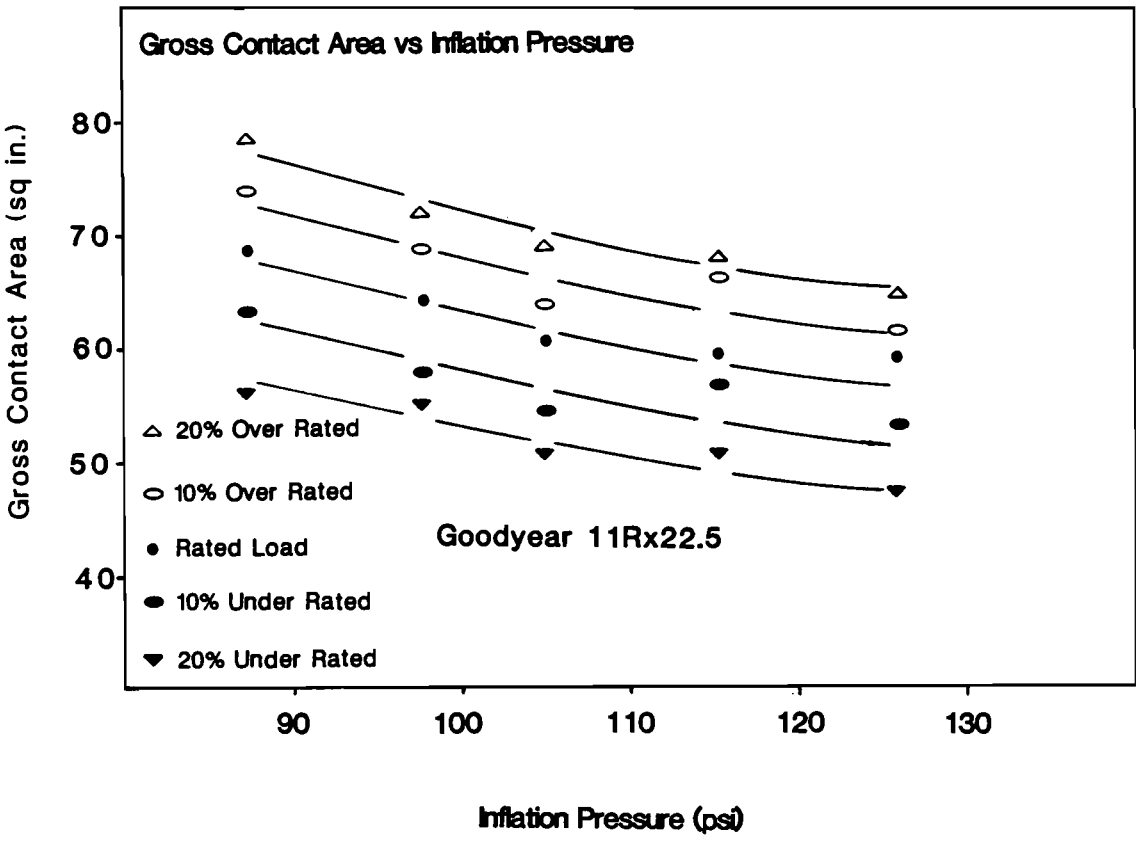

Fig. 2.3: Effect of Inflation Pressure on Gross Contact Area for Goodyear 11R-22.5

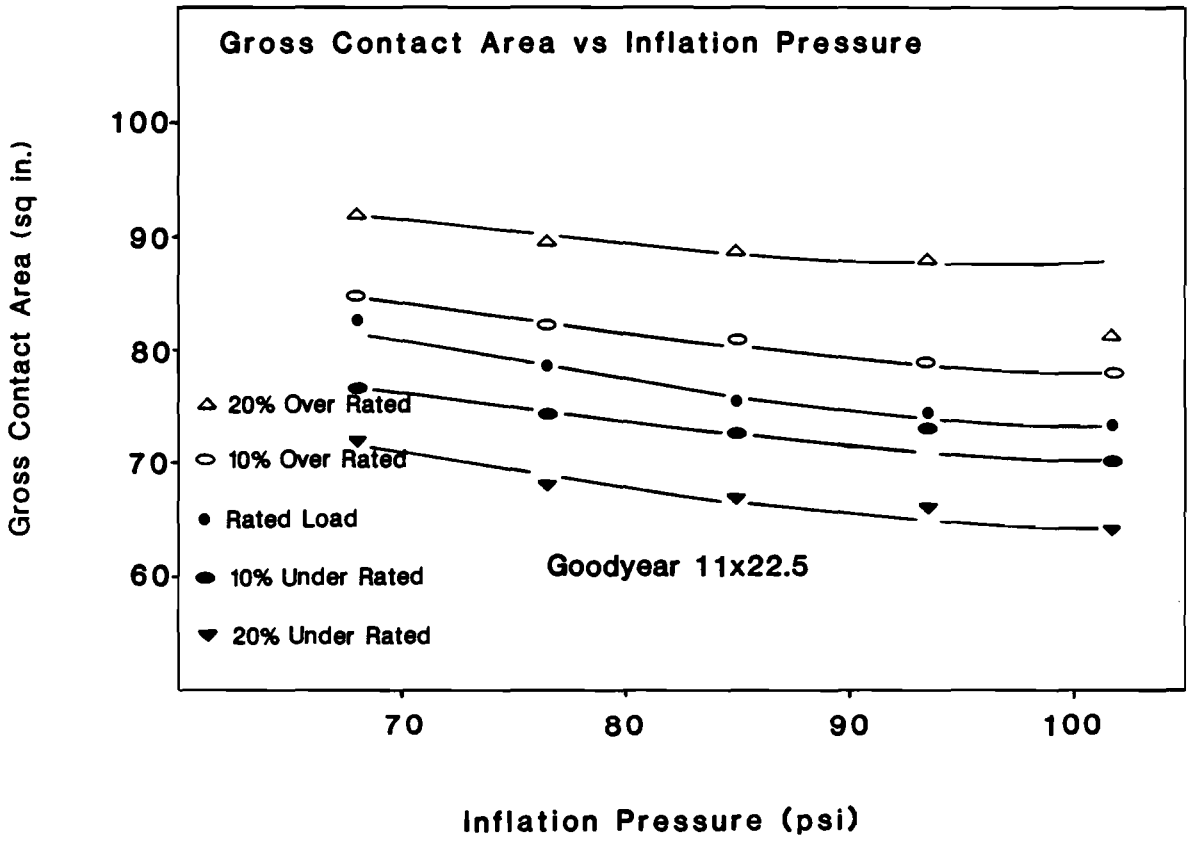

Fig. 2.4: Effect of Inflation Pressure on Gross Contact Area for Goodyear 11-22.5

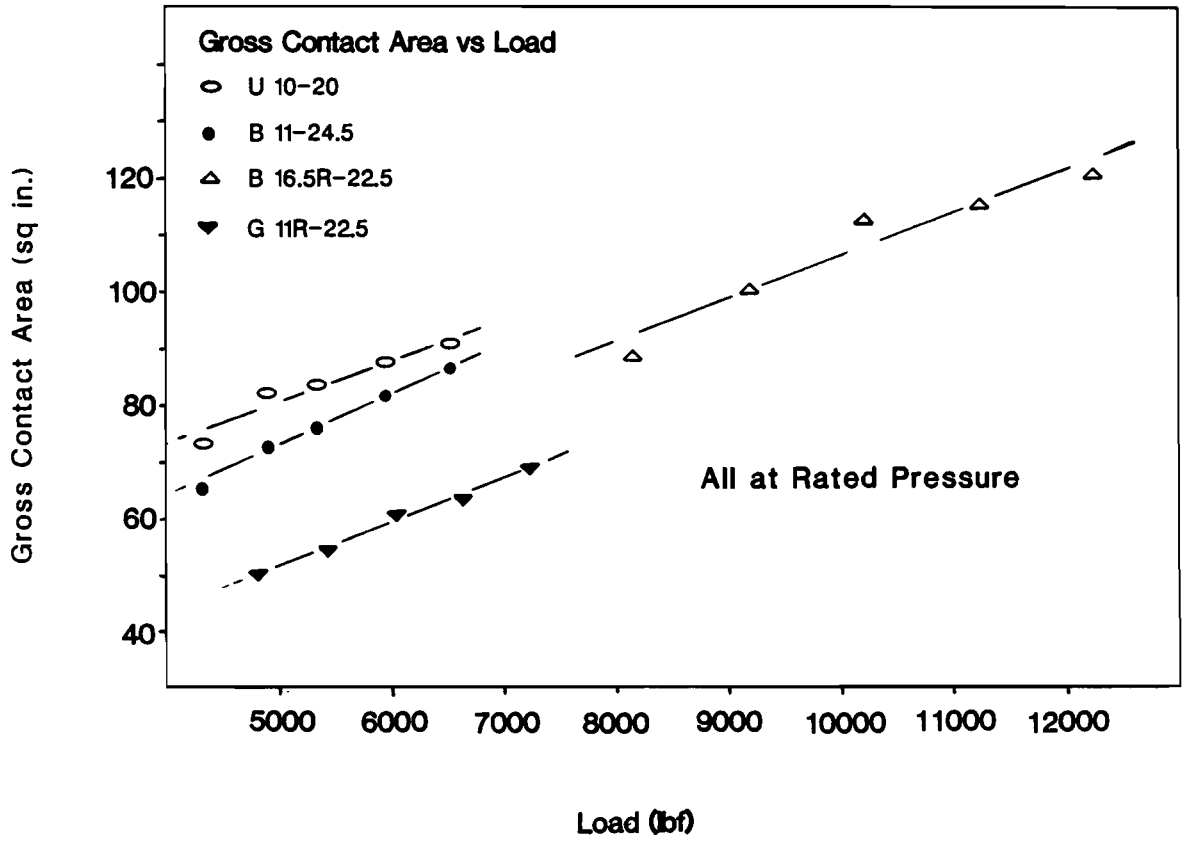

Fig. 2.5: Effect of Axle Load on Gross Contact Area

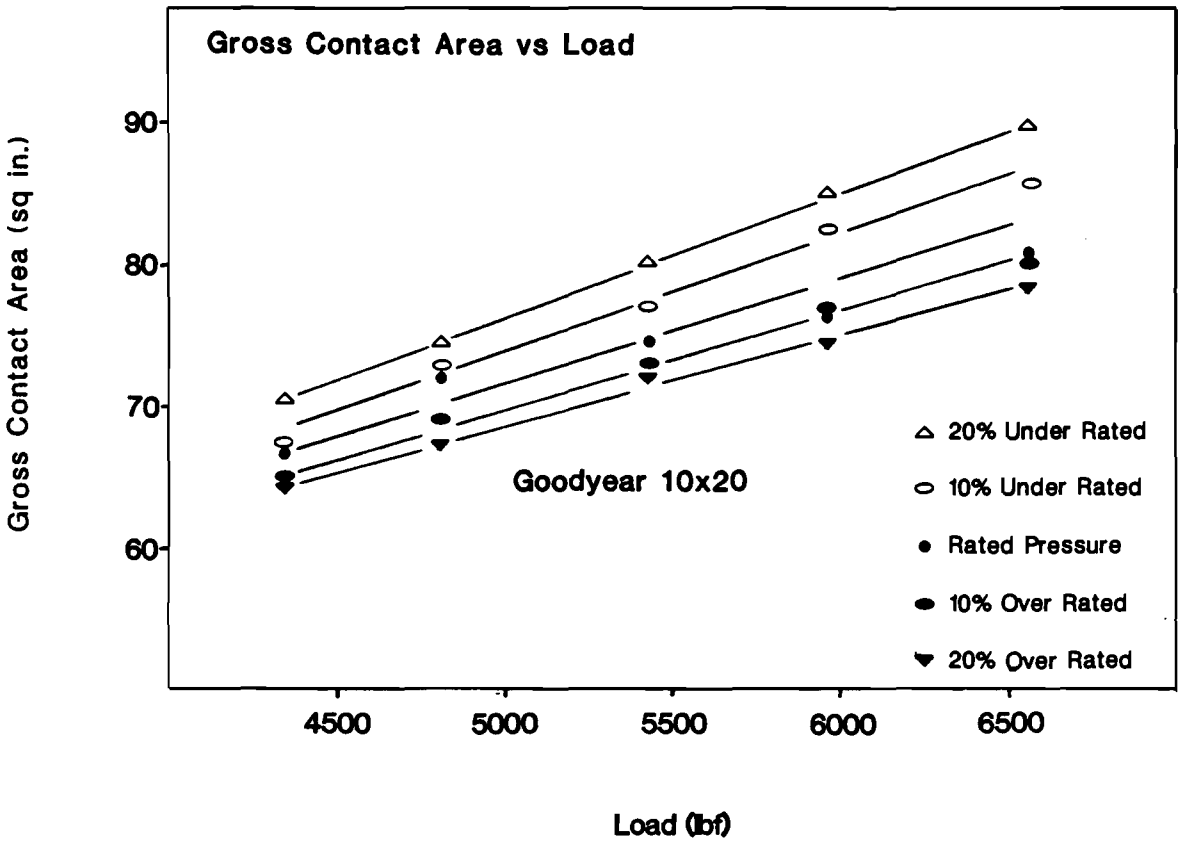

Fig. 2.6: Effect of Axle Load on Gross Contact Area for Goodyear 10-20

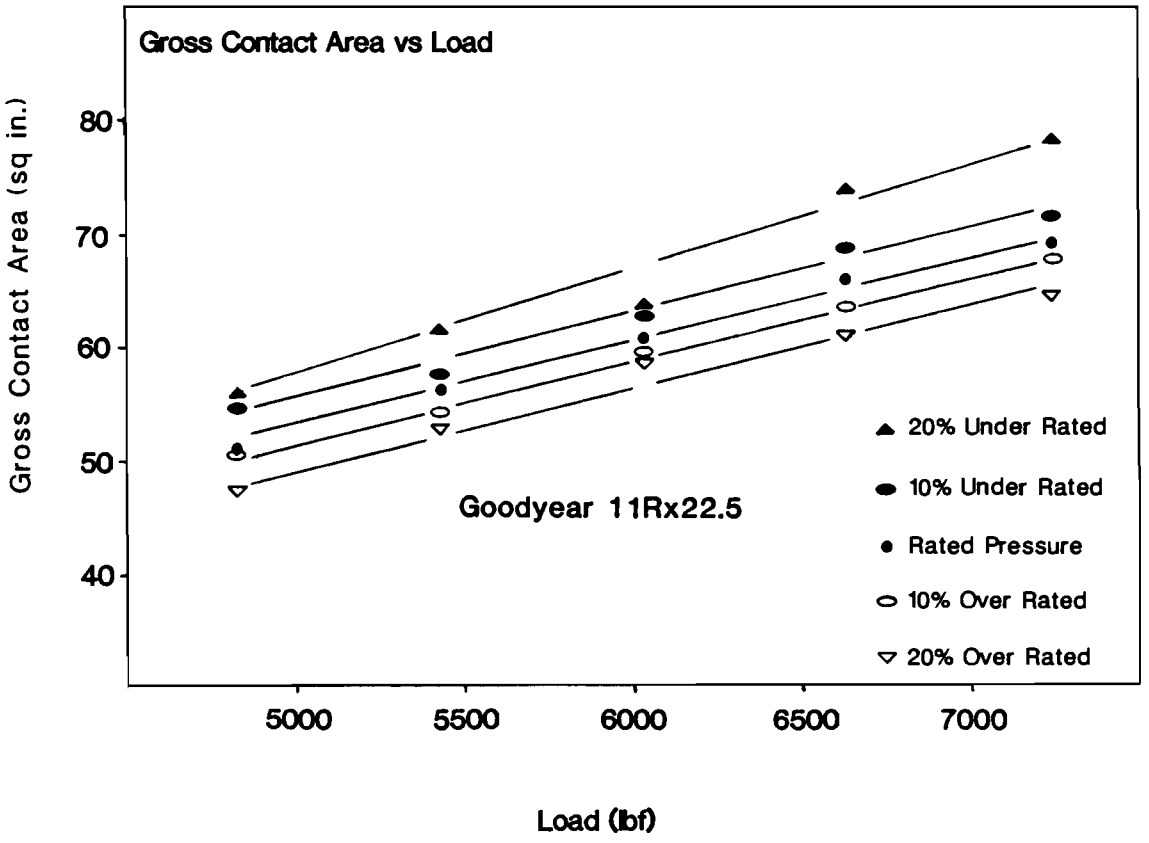

Fig. 2.7: Effect of Axle Load on Gross Contact Area for Goodyear 11R-22.5

2. An increased axle load produced a larger gross contact area. For an increase in axle load of 50%, there was a corresponding increase in gross contact area of approximately 30% to 35%.

3. Radial tires developed smaller contact areas than did bias ply tires; however, the rate of change in contact area with changes in tire inflation pressure and axle load for radial and bias ply tires was approximately equal.

CHAPTER 3. EXPERIMENTAL INVESTIGATION OF TIRE-PAVEMENT CONTACT PRESSURE DISTRIBUTIONS

This chapter discusses the experimental equipment and test procedures used to determine the contact pressure distributions beneath statically loaded truck tires (treaded and bald) using a pressure sensitive film. The principal objective was to determine what effects the tread pattern, tire inflation pressure, and axle load had on the resulting tire-pavement contact pressure distribution.

EXPERIMENTAL APPARATUS

The experimental apparatus used in this study consisted of the following components: a load frame for statically loading tires, pressure sensitive film for capturing the pressure distribution, an optical device (densitometer) for converting color intensity to pressure, a bi-directional (X-Y) table for precise movement of the print beneath the densitometer, and an HP 3054A data acquisition system.

Tires

The first tire studied was a smooth 10-20 bias ply truck tire used for skid testing purposes. The data from this tire will represent one extreme in the range of tread patterns found in use (as with a tire worn bald) and will thus allow broader conclusions to be drawn regarding tread patterns and the resulting pressure distributions. The second truck tire studied was a used 10-20 bias ply tire with 3/8 inch of tread depth remaining. This tire is representative of the type of tire and tire condition commonly found on highways today.

Load Frame

The truck tires were statically loaded with the load frame described in Chapter 2 and shown in Fig 2.1.

Pressure Sensitive Film

A pressure sensitive film was used which is capable of capturing the static pressure distribution between contacting bodies. The film consists of an A-sheet and a C-sheet, as shown in Fig 3.1, the A-sheet containing capsules of developer and the C-sheet providing a developing layer on which the developer acts. The capsules are made in a variety of sizes so that they break when exposed to a certain pressure level. Statistical distribution of the different capsule sizes allows a range of pressures to be captured.

When the two sheets are in their proper orientation and subjected to pressure, a number of the capsules break and release the developer onto the developing layer; the developer from the A-sheet produces a red spot on the C-sheet, with the intensity of color obtained being proportional to the applied pressure.

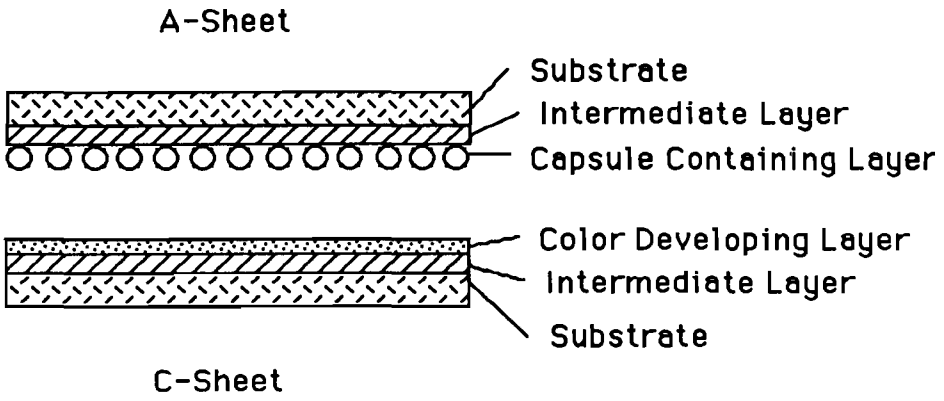

Fig 3.1 Pressure sensitive film

Densitometer

The developed prints are read with an optical device called a densitometer (shown in Fig 3.2). The densitometer consists basically of the reading head and a chassis that contains a voltmeter and calibration controls.

The reading head consists of two symmetrically placed light sources and a photocell. The light sources project beams of light which pass through a circular opening (0.118 inch in diameter) in the base of the head, striking the print directly below the head, and then reflecting back to the photocell an amount of light proportional to the intensity of color on the print. The photocell then outputs a voltage which is proportional to the pressure that was applied to the film; the response of the photocell is that of a first order system with a time constant of 0.8 second. The output of the densitometer photocell was connected to a precision voltmeter located in a data acquisition system.

The developed print can be read with the densitometer to determine the pressure at any point or region desired. One important advantage gained by using the densitometer is that a grid reading resolution can be specified, that is, the user can divide the resulting contact area into a grid size with step sizes as small or large as required. This characteristic is important since large pressure gradients occuring in extremely small distances are commonplace, especially when dealing with bodies such as treaded tires, whose contact surfaces contain numerous discontinuities.

X-Y Table

The small measuring area (0.044 square inch) of the densitometer compared with the large contact area of the truck tire footprint made it necessary to devise a means for automating the print reading process. This was accomplished in part through the use of a bi-directional (X-Y) table which featured high-speed, precision stepper motors driven by an onboard digital control unit. An RS232 interface in the control unit permitted direct control of the X-Y table and data taking by the HP 3054A data acquisition system described in the next section. The exclusive control of the HP 3054A over the data taking process avoided errors resulting from miscommunication between the densitometer and the X-Y table controller, and also kept the print reading time to a minimum.

Data Acquisition System

An HP 3054A data acquisition system was used extensively throughout all phases of this study. It consisted of the following components: an HP 9816S computer, a dual disc drive, a data acquistion unit, a dot matrix printer, and a multiple pen plotter.

Due to the small measuring area of the densitometer, roughly 6000 points were measured for each truck tire print in order to map the entire pressure distribution in the contact area. Fig 3.3 gives the schematic diagram of the print reading system.

EXPERIMENTAL PROCEDURE

The load application was divided into three parts. In the first part, the load on the tire was increased linearly from zero to full load over a two-minute time period. Part two of the loading consisted of maintaining the full tire load on the paper for two minutes. After this,the tire load was quickly released, the A-sheet was seperated from the C-sheet, and the C-sheet was set aside to finish developing. All prints obtained during a testing session were read within one hour after the session ended since it was thought that the color intensity on the film might fade with time.

To obtain a pressure print, the A and C sheets were taped firmly in their proper orientation to the flat steel plate to prevent erroneous pressure values from being recorded due to the presence of

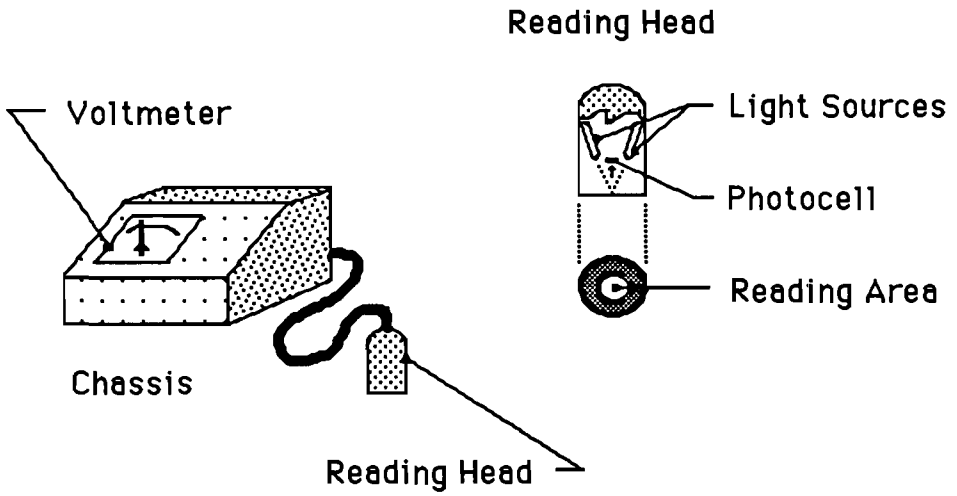

Fig. 3.2: Densitometer and schematic of densitometer reading head

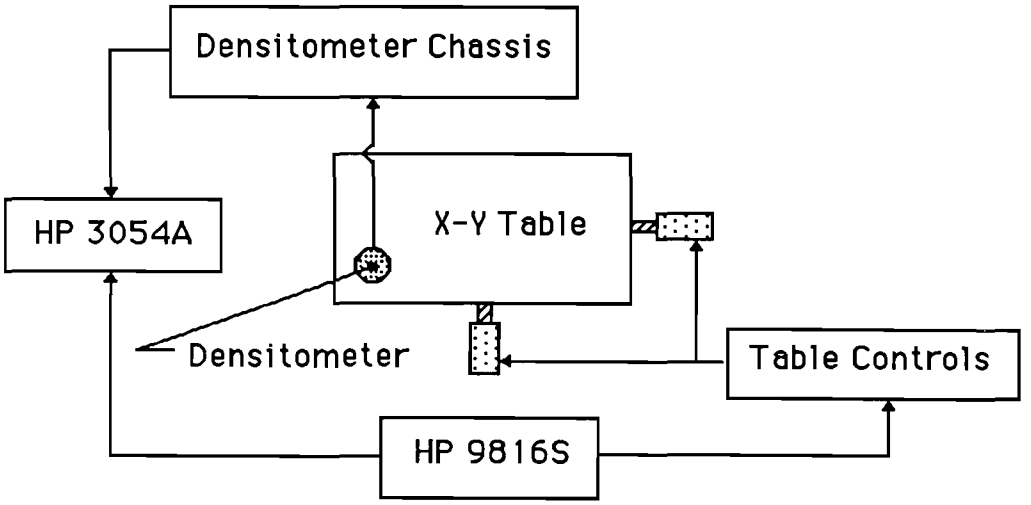

Fig 3.3: Print reading system

shear forces between the sheets. Also, a piece of shimstock (with a thickness of 0.001 inch) was placed between the tire and the top piece of pressure paper so that only the normal tire load was transmitted to the paper (see Fig 3.4).

To keep the calibration and experimental procedures as similiar as possible, a scheme was devised whereby a known load could be applied to a rubber cube with one inch sides (and a Young's modulus roughly equal to the moduli of the truck tires tested) using an Instron compression tester, as shown in Fig 3.5. Examples of calibration prints obtained with the rubber block and a complete description of the calibration procedure are given by Connell (Ref 9).

The data points used to construct the calibration curve were obtained using the same loading procedure as for the tire. The same steel plate and pressure sensitive film configuration was used, with the only difference being that the face of the rubber block touching the shimstock was lubricated to achieve a more uniform pressure distribution. The uniform distribution of known pressure intensity was desired for the calibration prints since the average voltage measured by the densitometer in each of these prints was used as a data point on the calibration curve.

Data points were obtained for each pressure level by averaging voltages in the calibration prints. A second order polynomial was fitted through the data points to obtain the calibration curve used to convert the voltage arrays to pressures (see Fig 3.6). Due to the sensitivity of the film to its environment, careful attention was paid to make sure that the atmospheric conditions (temperature and relative humidity) were sufficiently close for both calibration and experimental test sessions.

Experiments were conducted with truck tires to show the effect of tread pattern, tire inflation pressure, and axle load on the resulting contact pressure distribution. Since the pressure sensitive film is expensive, and since it required about six hours to read a developed print, the minimum number of tests were conducted which would satisfy the goals of this study.

Experiments were conducted using three different tire inflation pressures (75 psi, 90 psi, and 110 psi) to show what effect the inflation pressure had on the distribution of pressure in the tire footprint. Two different axle loads were used with this study; the first was a 4500 lbf load and the second was a 5400 lbf load (a 20% overload).

EXPERIMENTAL RESULTS

The data read by the densitometer from the six pressure prints was stored on disc in the form of arrays of voltages. From the voltage database, various parameters could be determined, including the net contact area of the tire footprint and the pressure distribution throughout. In addition, the data base could be reduced or converted into equivalent forms (such as equivalent but smaller arrays of pressures and forces); this made it possible to use the data (1) as a means of drawing pressure distributions, (2) to substantiate conclusions about the distribution, and (3) as input to computer programs analyzing pavement performance.

The first form of output used consists of numerical prints that show the pressure that acts on each grid area in the contact patch (see Fig 3.7 and Appendix A). A shorthand notation was developed to define the test parameters, for example, BALD 7545 indicates an experiment with the bald tire at an inflation pressure of 75 psi and an axle load of 4500 lbf. The numerical prints were made by printing the arrays of pressure values in matrix form. General trends in the pressure distribution are difficult to determine from the numerical prints, due to the overwhelming amount of data presented for each test conducted. The prints do, however, give the location of the pressure reading and the individual pressure values that exist in the contact patch. The experimental data for maximum contact pressure, contact area, and percent difference between the experimental data (force summation) and actual applied load is shown in Appendix B.

A number of operations were performed on the data to reduce it from an array of 6000 points (either pressure or force) per print to a smaller number of points appropriate to the application. In

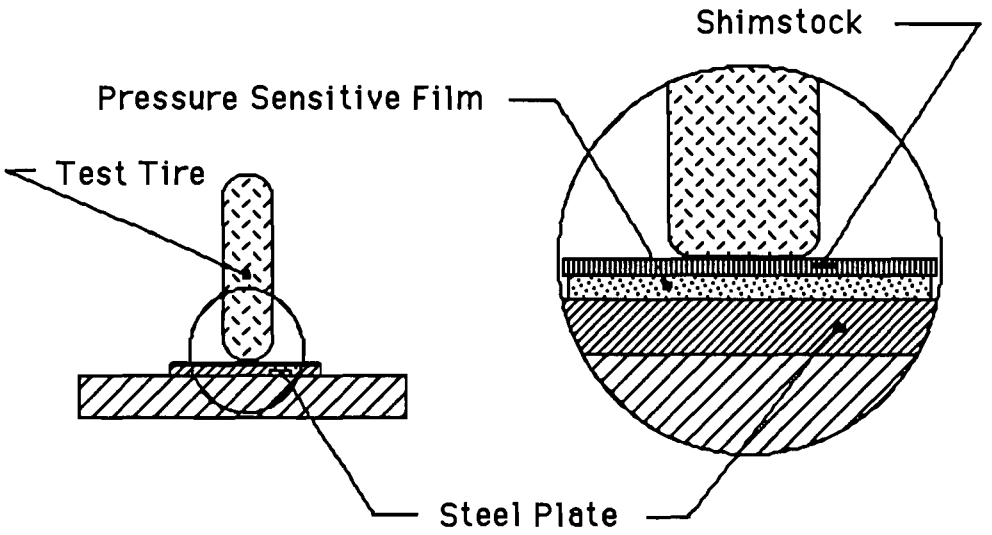

Fig 3.4: Shimstock and pressure sensitive film configuration

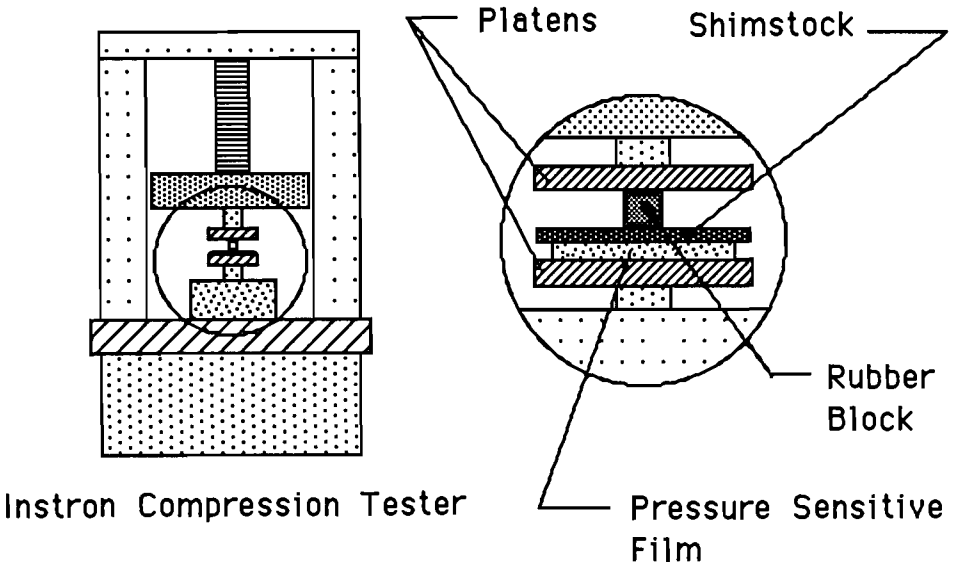

Fig 3.5: Calibration test equipment

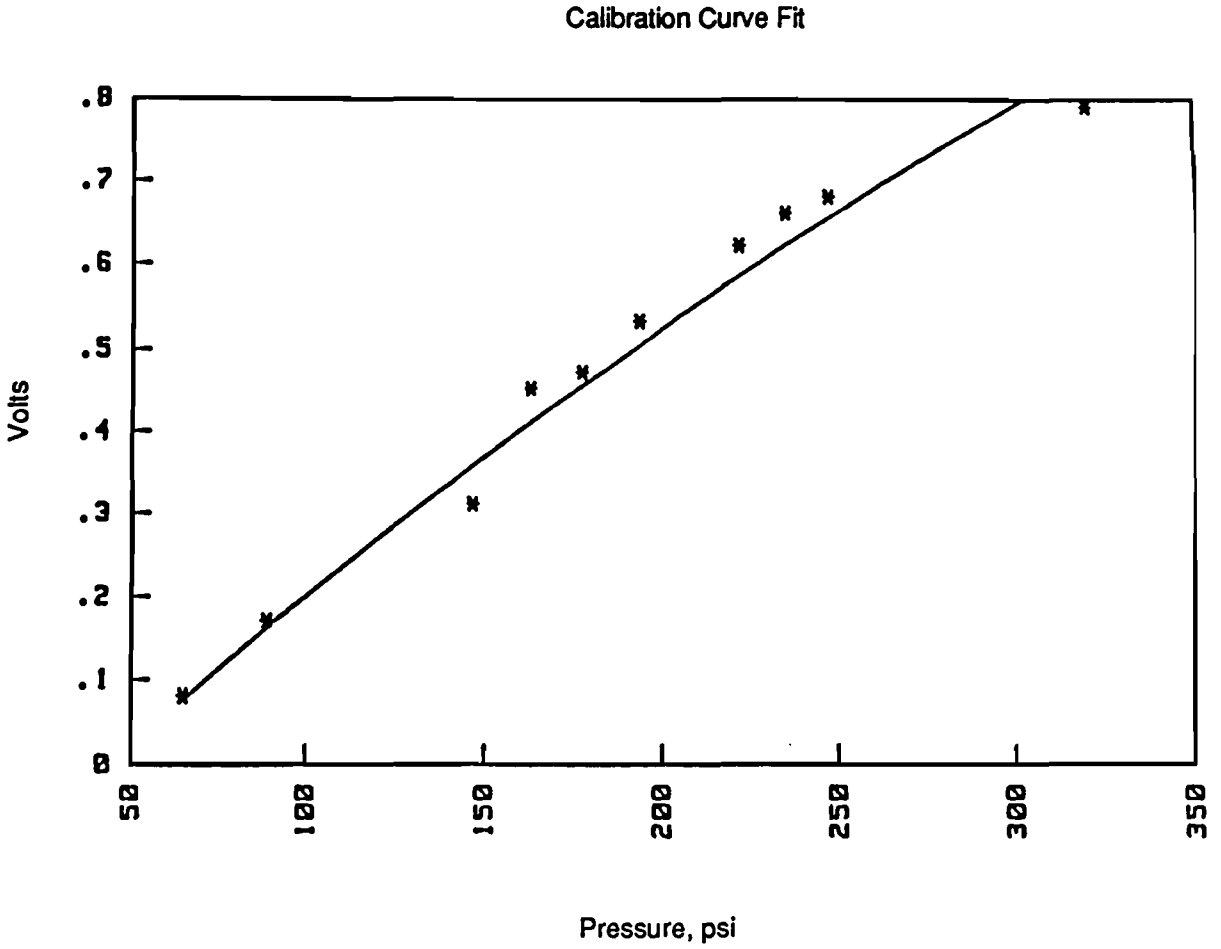

Fig. 3.6: Calibration curve for rubber block

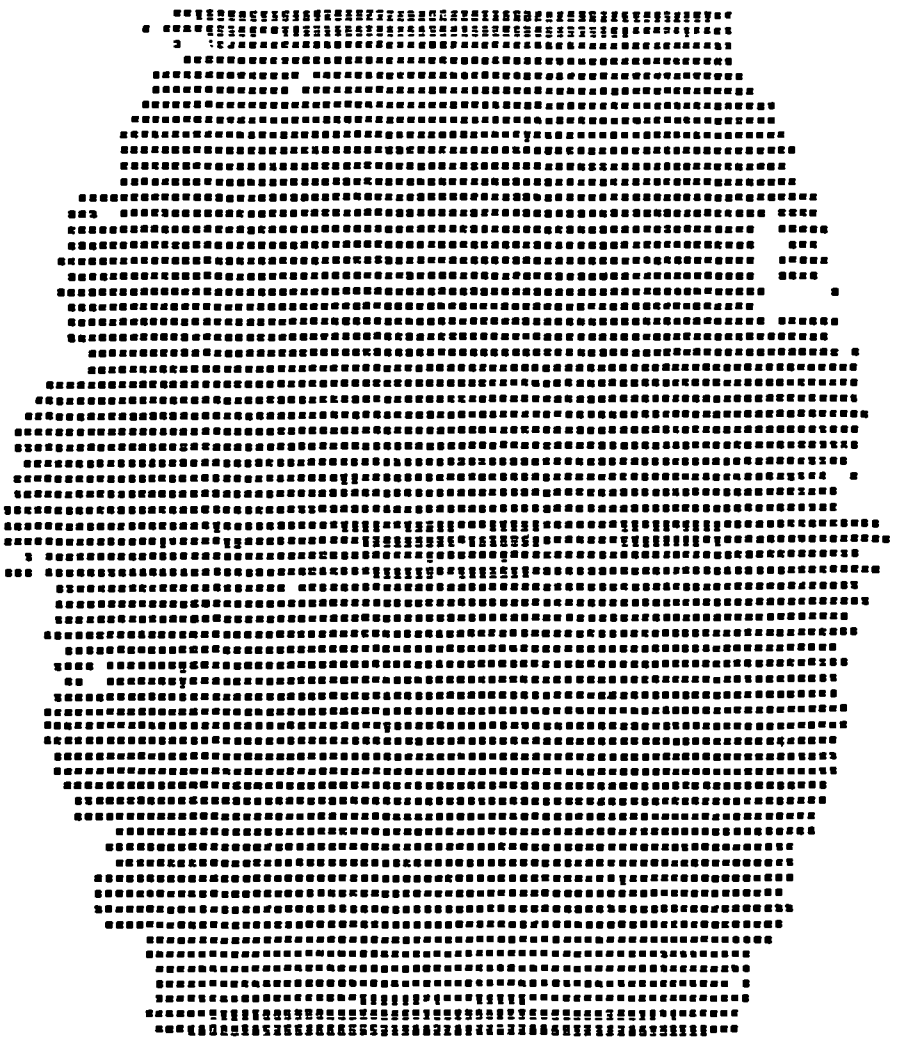

Fig. 3.7: Numerical contact pressure print for BALD 7545

general, the operations on the data were performed to accomplish one of two goals: the first goal was to reduce the data to a form suitable for plotting, and the second was to convert the data to an equivalent form compatible with the input requirements of pavement analysis programs.

A 3-dimensional plot was chosen over a 2-dimensional plot despite the usual assumption that the pressure distribution varies little along the tire length (in the direction of travel). The 3-dimensional plots were rotated so that the view chosen best illustrates the pressure profiles along both axes of the footprint (see Fig 3.8).

The grid dimensions used to make the 3-dimensional plots were made non-uniform in order to preserve areas of high pressure that were isolated due to the presence of the tire shoulder or a tread gap. A moving average scheme was then used to reduce the data to obtain a single pressure or force acting on each unit area. The plots given in Fig 3.8 optimize the viewing variables so that one can clearly see the pressure changes in the contact patch along the two axes and the presence of high pressures at the tire shoulder and along tread gaps.

A computer graphics program was used to convert each database of numerical pressure values into discrete points of color on a graphics terminal; controls in the graphics program associated a particular pressure level with a specific color (for example, yellow points might indicate pressures between 120 and 140 psi). After the entire database for each print had been read into the graphics program, plots on the color graphics terminal were photographed with a 35 mm camera. Prints made from the slides give a striking summary of the experimental results, showing both the localized pressures and the general trends in pressure found in the contact patch beneath statically loaded truck tires. Prints of the 35 mm slides are given in Ref 9.

DISCUSSION OF RESULTS

The tread type, that is, the particular pattern of treads, plays a dominant role in the determination of the shape of the pressure distribution. The bald tire represents one end of the tread spectrum, the treaded tire the other. The plots shown in Fig 3.8 illustrate that a bald tire produces a uniform pressure distribution with significant gradients only at the tire center and the shoulder.

With a treaded tire, the pressure distributions have large discontinuities at the tread gaps, within which the pressure is zero. The gaps seperate regions of signficantly different non-zero pressure levels. This is clearly seen on the copies of the pressure prints (see Appendix A), especially for the overloaded case (treaded tire at 90 psi and 5400 lbf) where the circumferential tread gap seperates high pressures on the shoulder from medium pressures directly on the other side. This region between the shoulder of the tire and the circumferential gap usually carries the highest pressures.

For a given load, inflation pressure determines the regions of high pressure. Increasing the inflation pressure reduces the crown curvature, thus shifting the high pressure regions at the tire shoulder to the center of the contact patch.

One other effect of inflation pressure was observed with the treaded tire that supports the use (by highway engineers) of the inflation pressure as the magnitude of the uniform pressure delivered by a tire. The region in the center of the tire, bounded by a circumferential gap on either side, consistently maintained localized pressures close to the inflation pressure (plus or minus 15 psi) for all the tests conducted. The high pressures occurred near a tread gap or in the shoulder region where the stress consentration drove the pressures above the range stated.

The axle load is the final parameter whose effect on the contact pressure distribution was studied. A comparison of the numerical and 3-dimensional plots obtained for the treaded tire at rated inflation pressure but for two different axle loads immediately makes clear the following: the pressures in the center region of the tire remain relatively unchanged whereas pressures in the shoulder region increase dramatically.

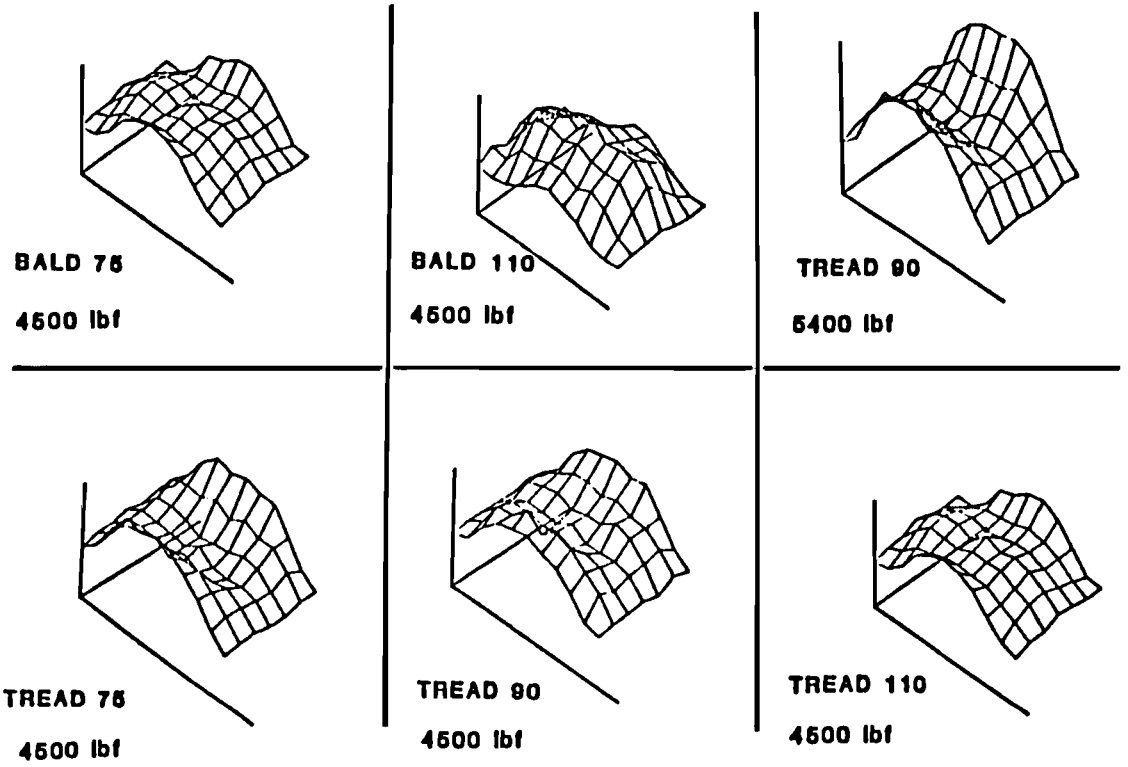

Fig. 3.8: 3-Dimensional plots of pressure distribution

CONCLUSIONS

The conclusions of this study can be summarized as follows:

(1) The tread pattern on a tire was found to have a significant effect on the size of the contact area and the shape of the pressure profiles. Smaller contact areas for treaded tires were observed since the presence of the tread gaps reduced the number of contact points in the tire footprint. The tread gaps were also shown to seperate adjacent regions of vastly different pressure levels. High pressures were consistently found at tread-gap interfaces and at the tire shoulder. As the tread wears, one can expect an increase in the net contact area, and a reduction of the peak pressures (along with a more continuous distribution).

(2) The tire inflation pressure, in general, determined the location of regions of high pressure in the contact patch. Low inflation pressures resulted in large contact areas and high pressures near the tire shoulder region. High inflation pressures produced a significant reduction in contact area and a shifting of high pressures towards the center region of the contact patch.

(3) The axle load also affected the contact area and pressure distribution. The 4500 lbf axle load saturates the center region of the tire footprint with localized contact pressures approximately equal to the tire inflation pressure. The 5400 lbf axle load caused deformations in the tire sidewalls and an increase in the load carried by the tire shoulder region.

CHAPTER 4. CONCLUSIONS AND RECOMMENDATIONS

SUMMARY OF CONCLUSIONS

Based on the limited number of cases investigated, the conclusions of this study can be summarized as follows:

(1) Statically loaded tires produce smaller gross contact areas with increases in inflation pressure. For a 50% increase in tire inflation pressure, there was (approximately) an 8% to 20% decrease in the gross contact area.

(2) Statically loaded tires produce larger gross contact areas with increases in axle load. A 50% increase in axle load produced approximately a 25% to 35% increase in the gross contact area.

(3) Radial tires develop smaller gross contact areas than do bias ply tires, but the rates of change in contact area with changes in tire inflation pressure and axle load for the two tire types are approximately equal.

(4) The tread pattern on a tire was found to have a significant effect on the size of the net contact area and the shape of the pressure distribution. Smaller net contact areas for treaded tires were observed since the presence of the tread gaps reduced the amount of contact in the tire footprint. The tread gaps were shown to seperate adjacent regions of different pressure levels and to act as stress raisers, as demonstrated by the high pressures consistently found along the edges of the tread-gap interfaces and at the tire shoulder. As the tread is worn off a tire, one can expect an increase in the net contact area and a reduction of the peak pressures near the tire shoulder (along with a more continuous pressure distribution).

(5) The tire inflation pressure, in general, determined the rate of growth of the net contact area and the location of regions of high pressure in the contact patch. The treaded tire (with an inflation pressure 20% under rated) produced net contact areas 4% larger than those produced by the tire at rated inflation pressure. The treaded tire at 110 psi inflation pressure (20% over rated) produced a net contact area 1% smaller than that produced by the tire at rated inflation pressure and shifted regions of high pressure from the tire shoulder region towards the center of the contact patch. In addition, the inflation pressure influenced the amount of load that will have to be carried by the shoulder region; high inflation pressures required the shoulder to carry lower peak loads since the localized pressures beneath the majority of the tire center region were all close to the inflation pressure.

(6) The axle load also affected the rate of net contact area growth and the shape of the contact pressure distribution. For an increase in axle load of 20% there was a corresponding increase of 10% in the net contact area for the Goodyear 10 x 20 bias ply truck tire. At an axle load of 4500 lbf, the region under the center of the tire was

saturated with pressures close to the inflation pressure, with the peak loads being carried in the tire shoulder region. An increase of 20% in the axle load had little effect on the pressures under the center region of the tire but caused the shoulder region to be saturated with pressures between approximately 160 and 220 psi.

RECOMMENDATIONS

The following recommendations are made for future research on tire contact pressure distributions:

(1) Conduct experiments on a variety of bias ply and radial car and truck tires in order to develop a general pressure distribution model (for pavement design work) that better represents the actual contact pressure distribution.

(2) Develop a technique to measure the tire-pavement contact pressures that exist for tires loaded on actual pavement materials which have surface irregularities and surface debris.

(3) Conduct experiments on tires at various driving speeds to determine what effect the vehicle dynamics have on the resulting contact pressure distribution.

REFERENCES

1. Woods, Kenneth B., Editor, Highway Engineering Handbook, New York: McGraw-Hill, 1960.

2. Flugrad, Donald R., and Bruce A. Miller. "Experimental and Finite Element Study of a Standing Torus Under Normal and Tangential Loads." Iowa State University, 1981.

3. Mack, Micheal J., Jr, Daniel E. Hill, and Joseph R. Baumgarten. "Analytical and Experimental Study of a Standing Torus with Normal Loads." Tire Modeling, NASA Conference Publication 2264, 1982.

4. O'Neil, Ernest W., Jr., Measurement of Pneumatic Tire Contact Pressure for Static Loading, M.S. Thesis, North Carolina State University, 1969.

5. Tielking, J.T., "A Finite Element Tire Model," Tire Science and Technology, Vol. II, Nos. 1-4, January-December, 1984, pp. 50-63.

6. Lippmann, S.A., and K.L. Oblizajek. "The Distribution of Stress Between the Tread and Road for Freely Rolling Tires." S.A.E. Transaction 740072, 1974.

7. Shimada, T., S. Furuya, and K. Ikehara. "A Study of Contact Forces of a Radial Tire at High Speed." Akron, Ohio: Bridgestone Tire Company, Inc., 1984.

8. Grinnell User's Manual, GMR-27, GSC-100599B, Grinnell System Corporation, San Jose, California.

9. Connell, R.B., Experimental Determination of Truck Tire Contact Pressures and Their Effect on Flexible and Rigid Pavement Performance, M.S. Thesis, The University of Texas at Austin, 1985.

10. Clark, Samuel K., Editor, Mechanics of Pneumatic Tires, Washington, D.C.: U.S. Department of Transportation, 1975.

APPENDIX A

COPIES OF PRESSURE PRINTS AND NUMERICAL PRESSURE DISTRIBUTIONS

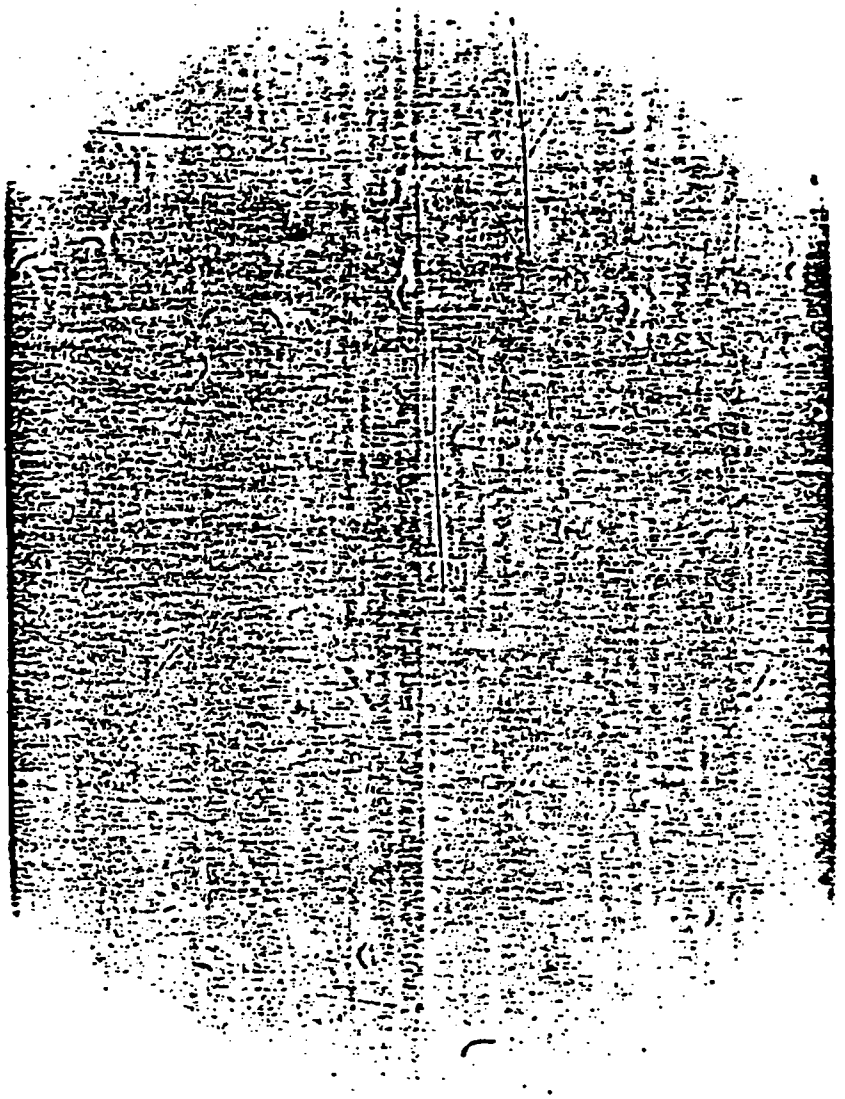

Fig. A.1. Pressure print for Bald 7545

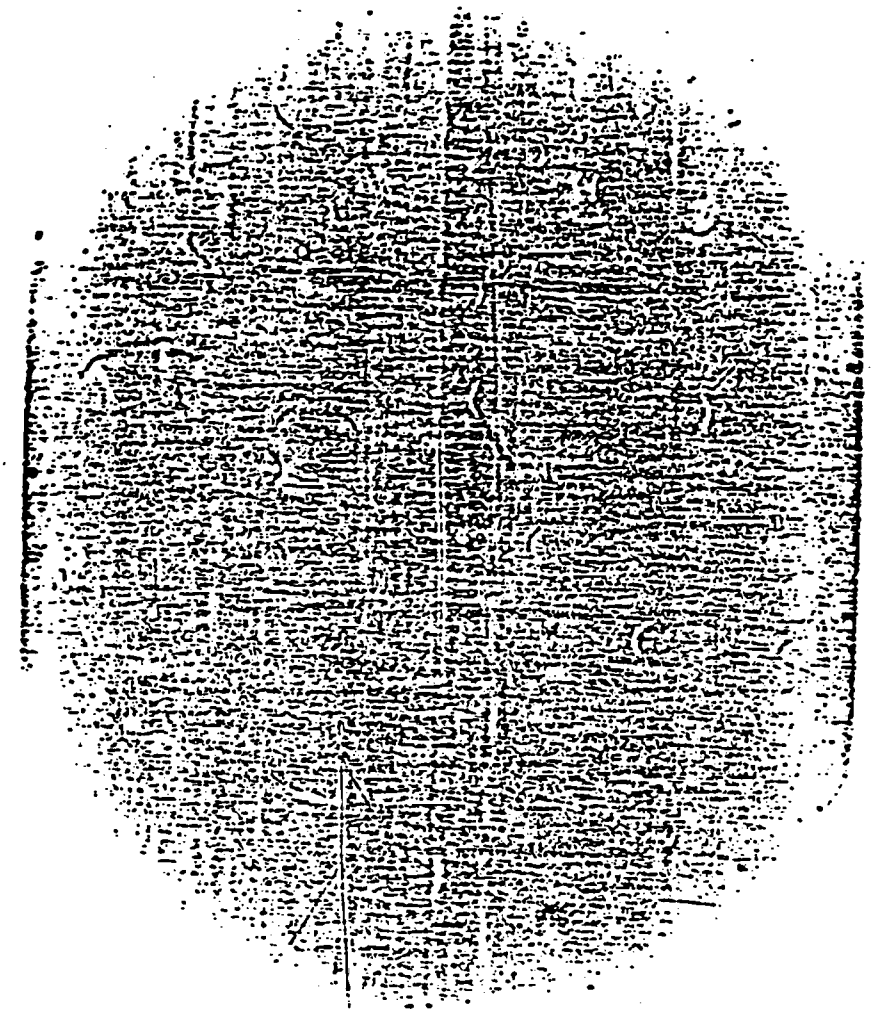

Fig. A.2. Pressure print for Bald 11045

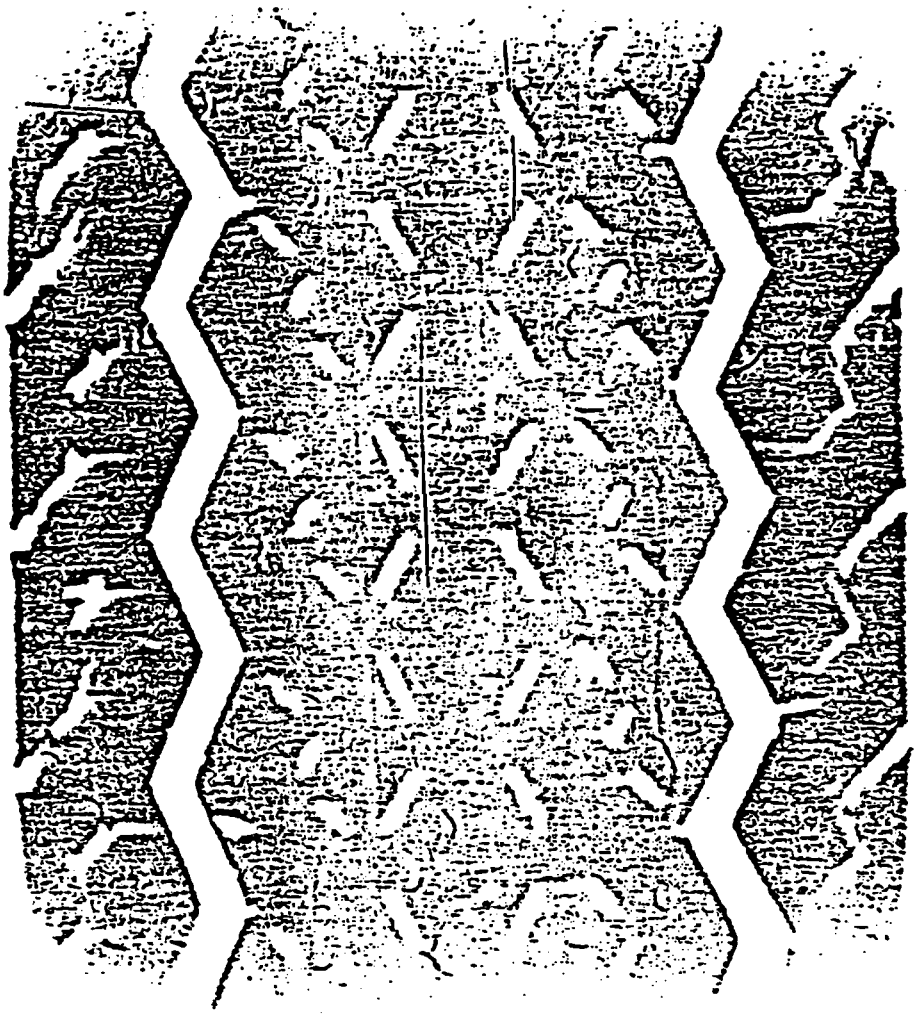

Fig. A.3. Pressure print for Tread 7545

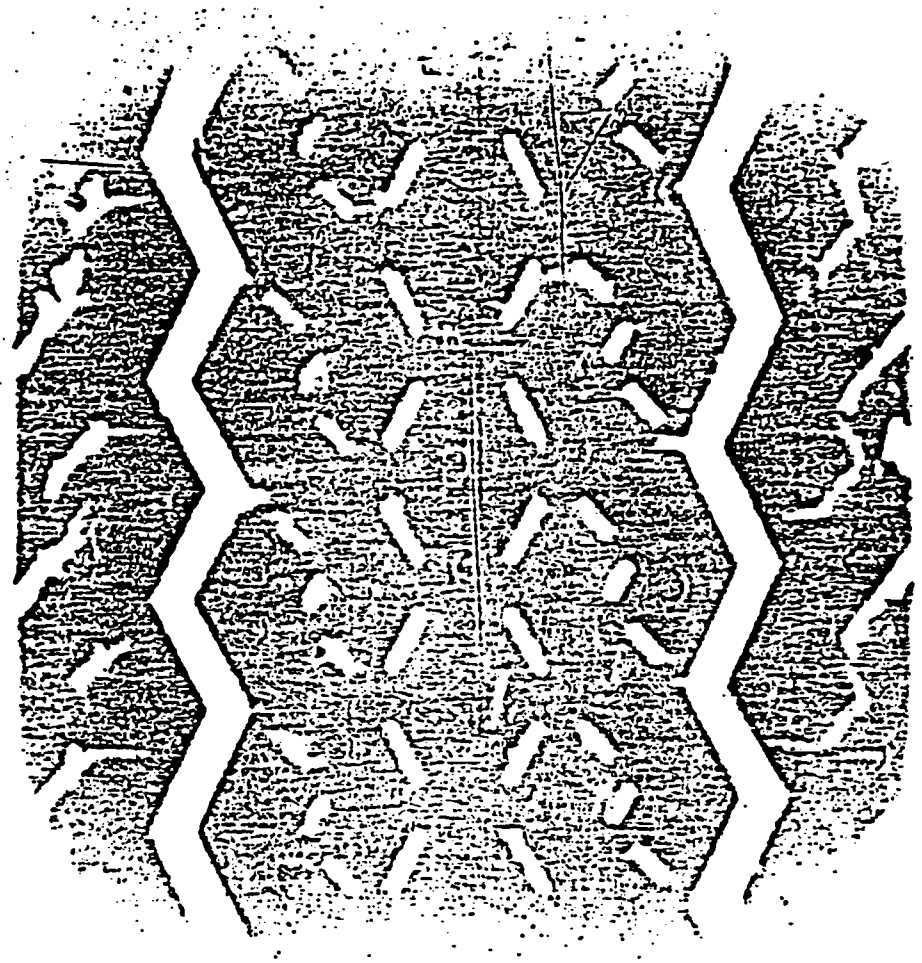

Fig. A.4. Pressure print for Tread 11045

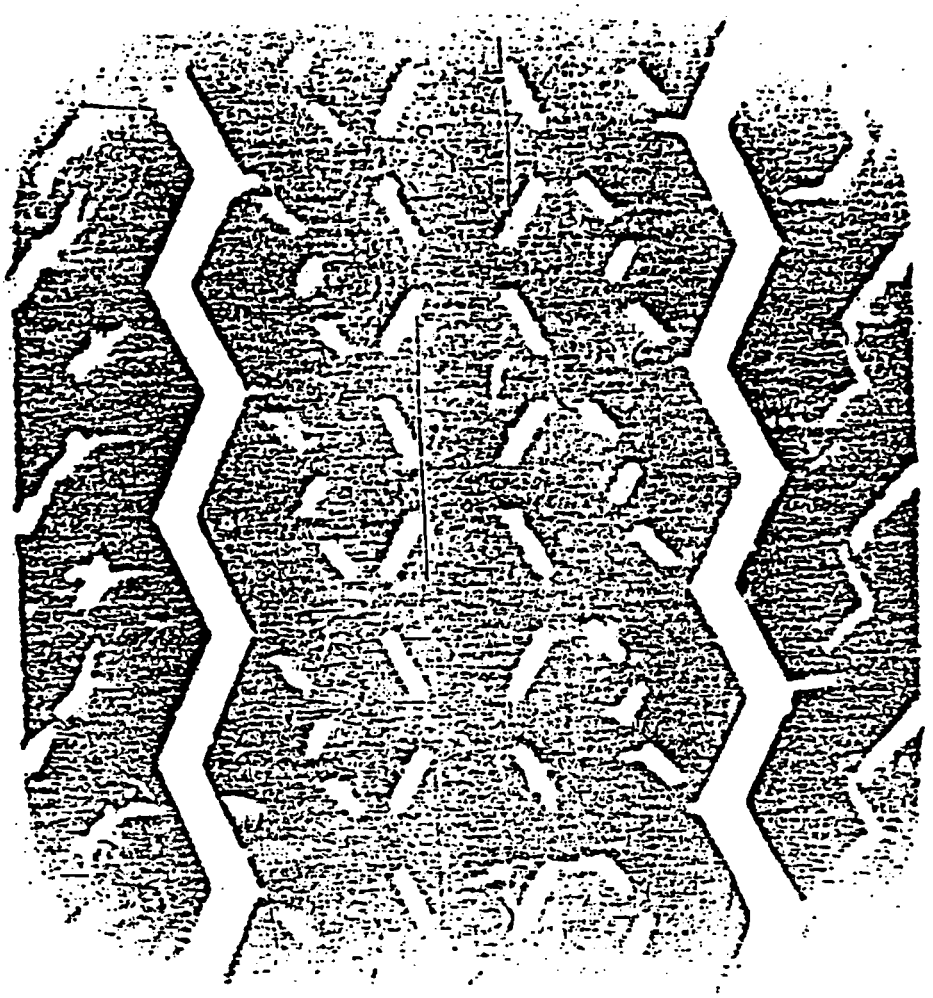

Fig. A.5. Pressure print for Tread 9045

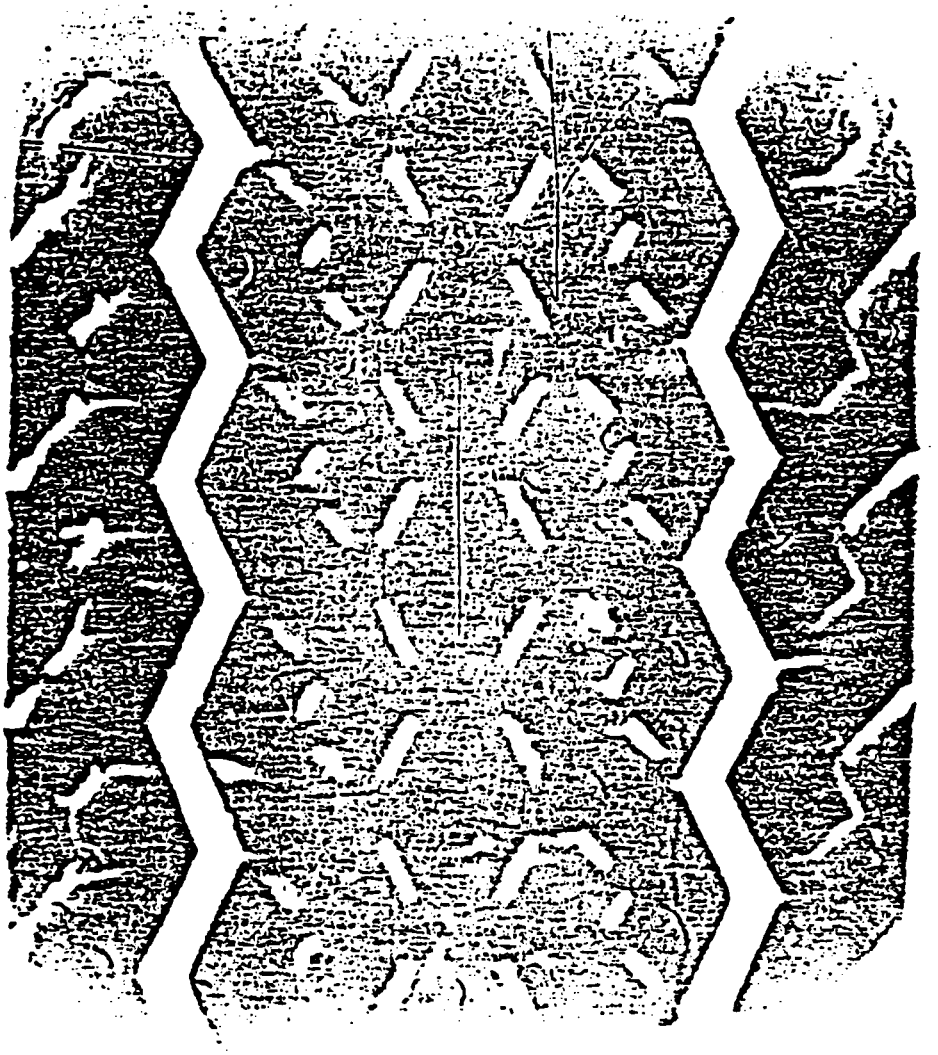

Fig. A.6. Pressure print for Tread 9054

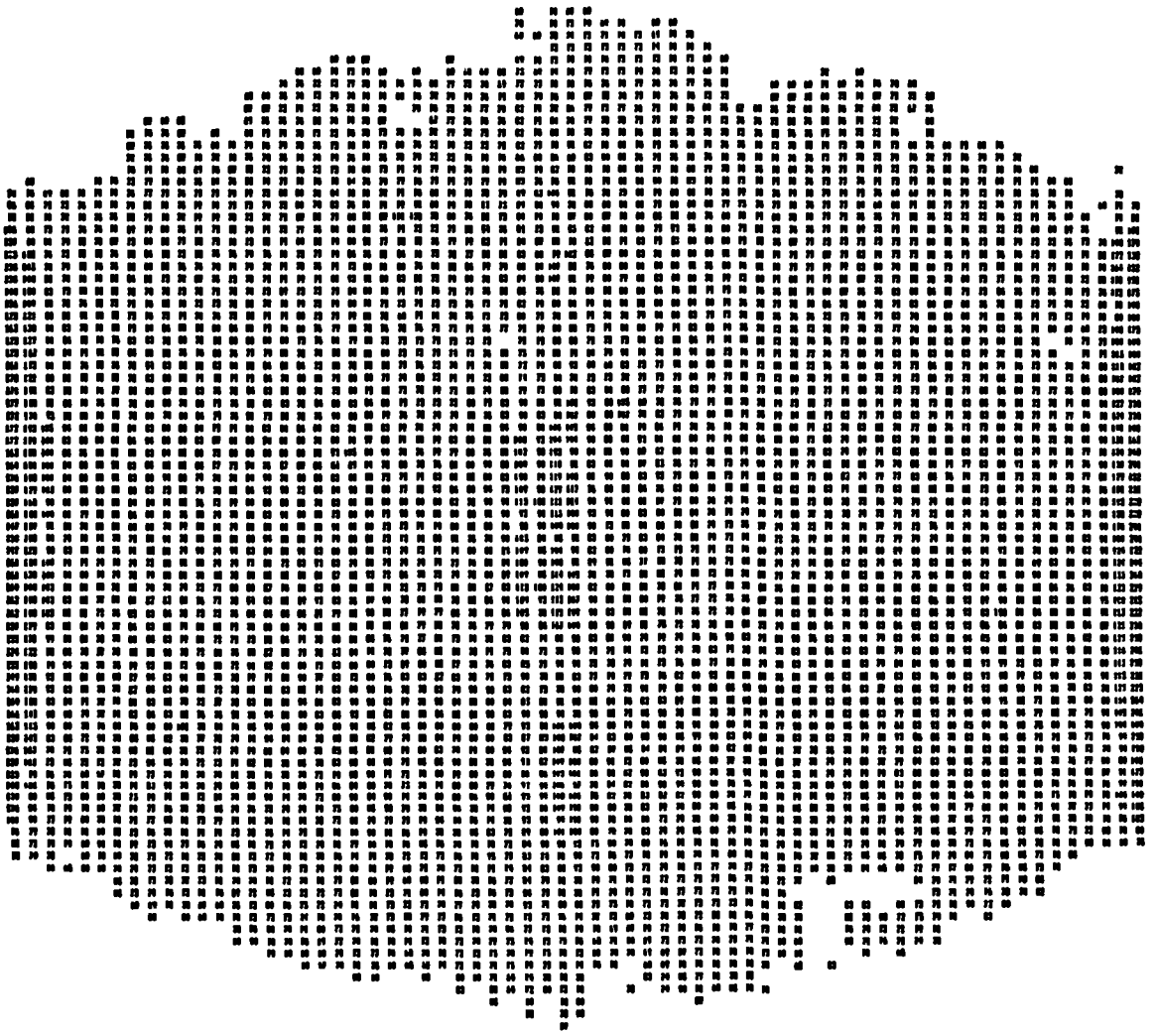

Fig. A.7. Numerical contact pressure print for Bald 7545

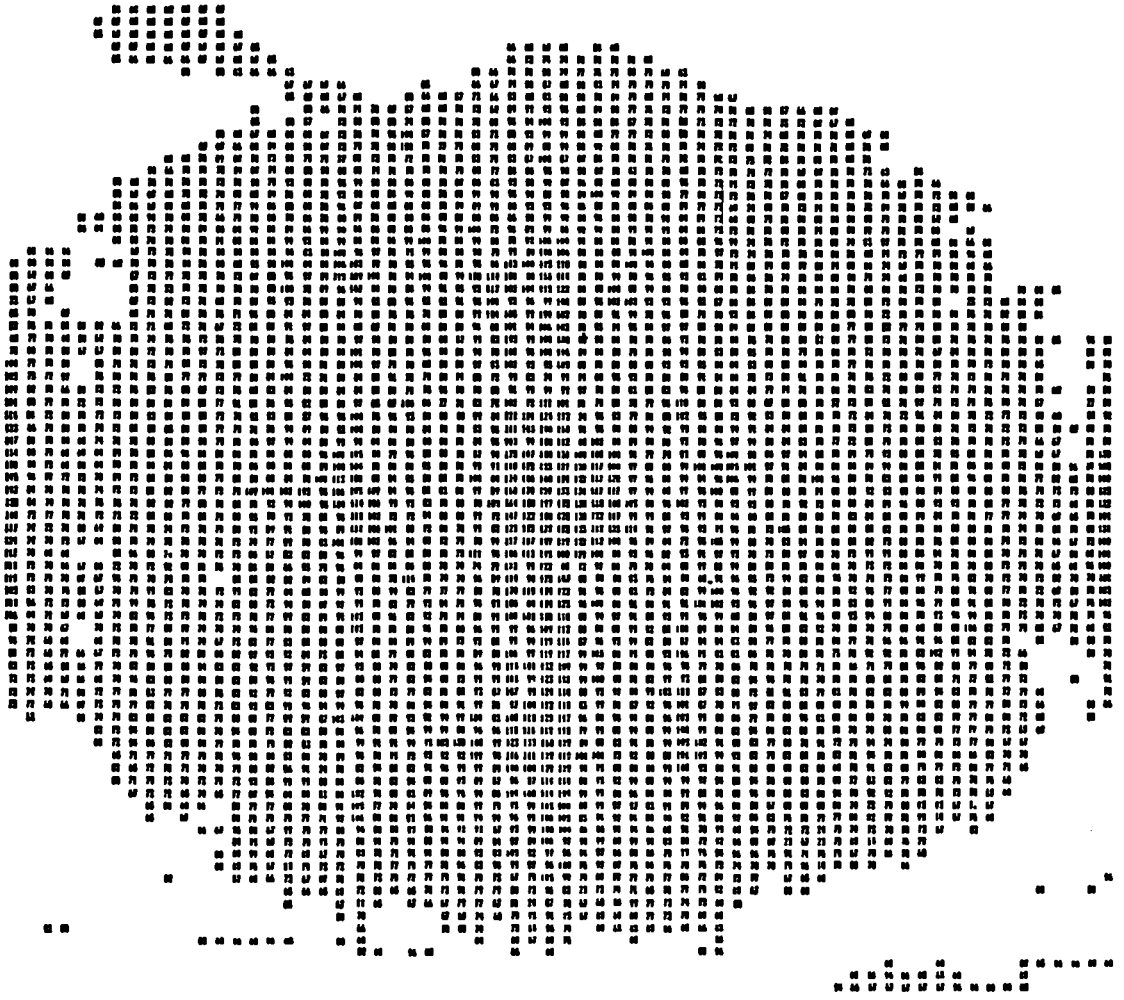

Fig. A.8. Numerical contact pressure print for Bald 11045

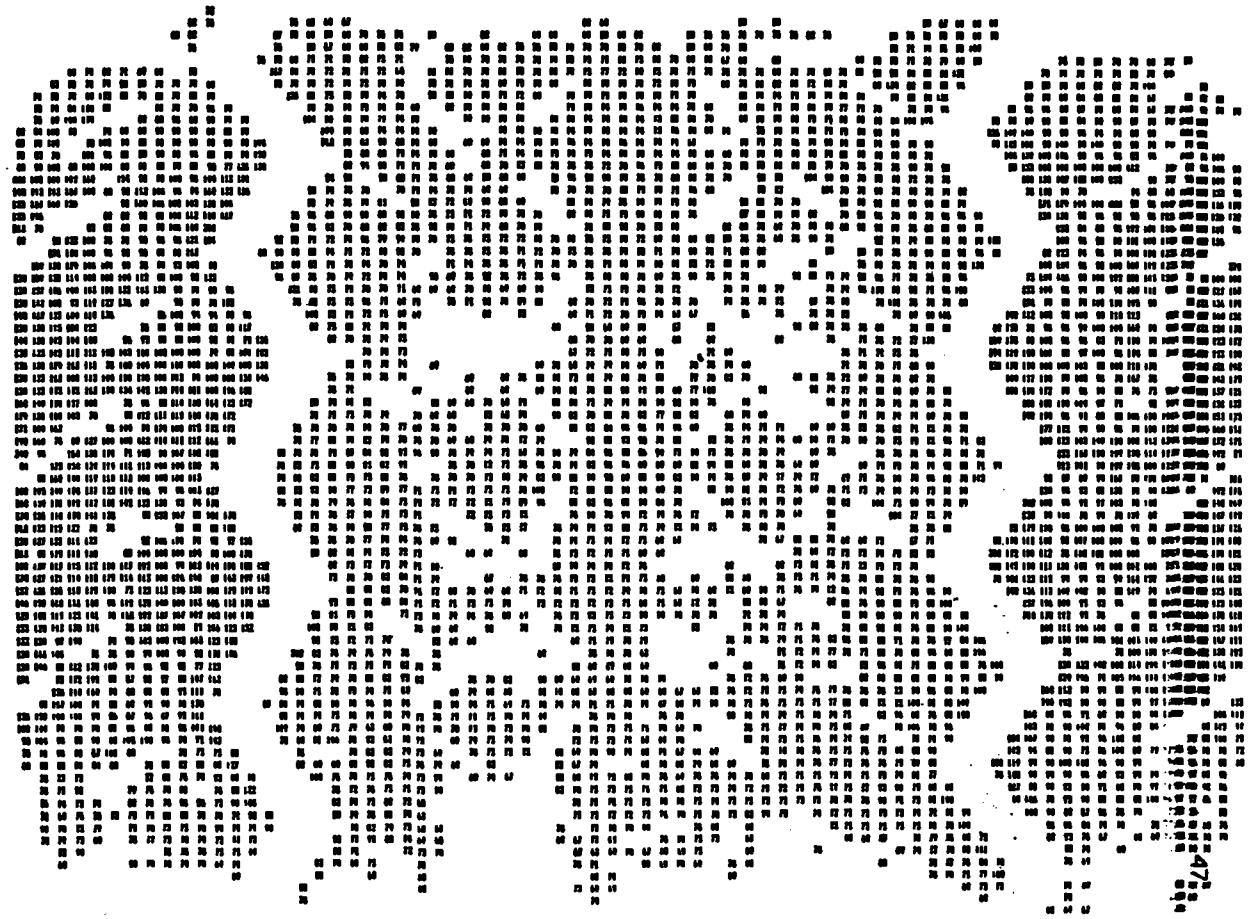

Fig. A.9. Numerical contact pressure print for Tread 7545

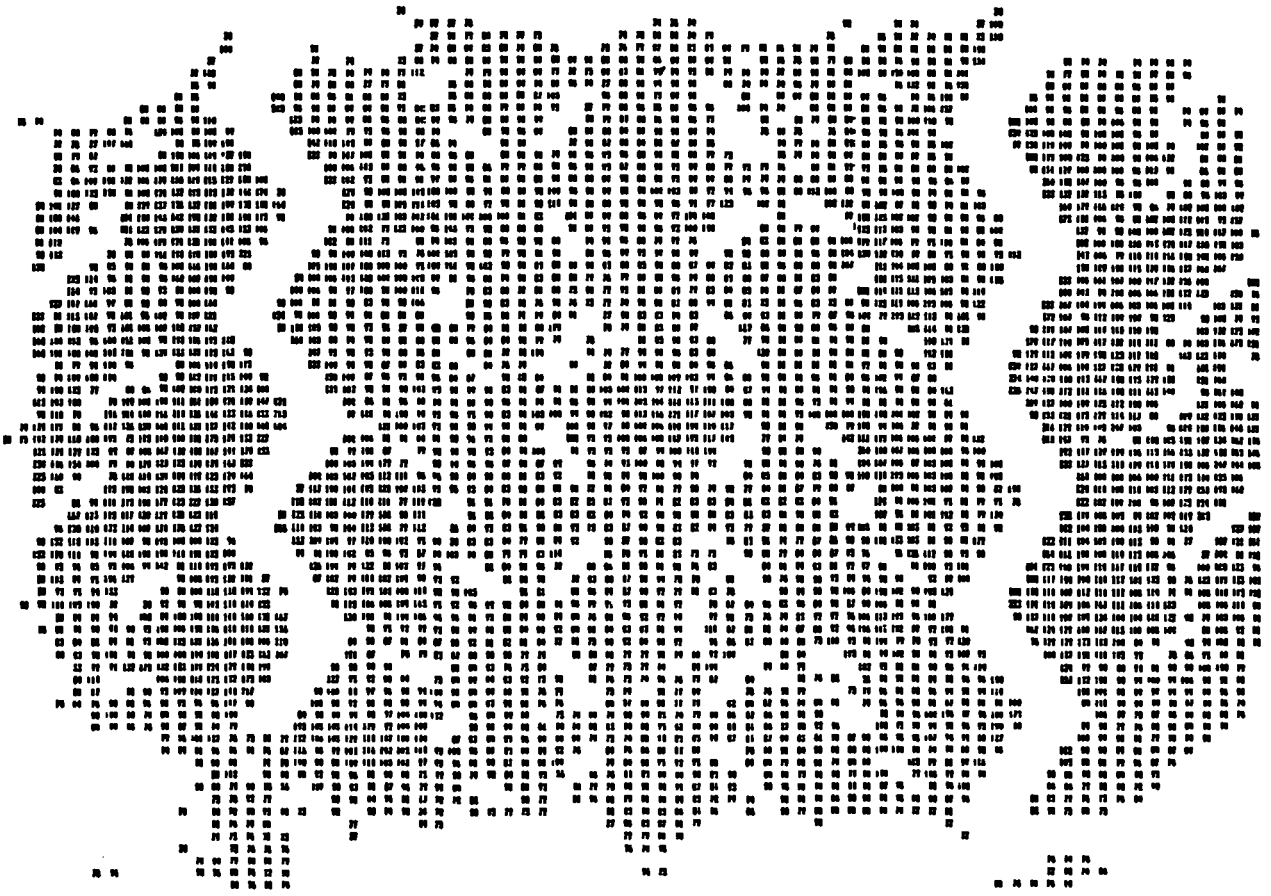

Fig. A.10. Numerical contact pressure print for Tread 11045

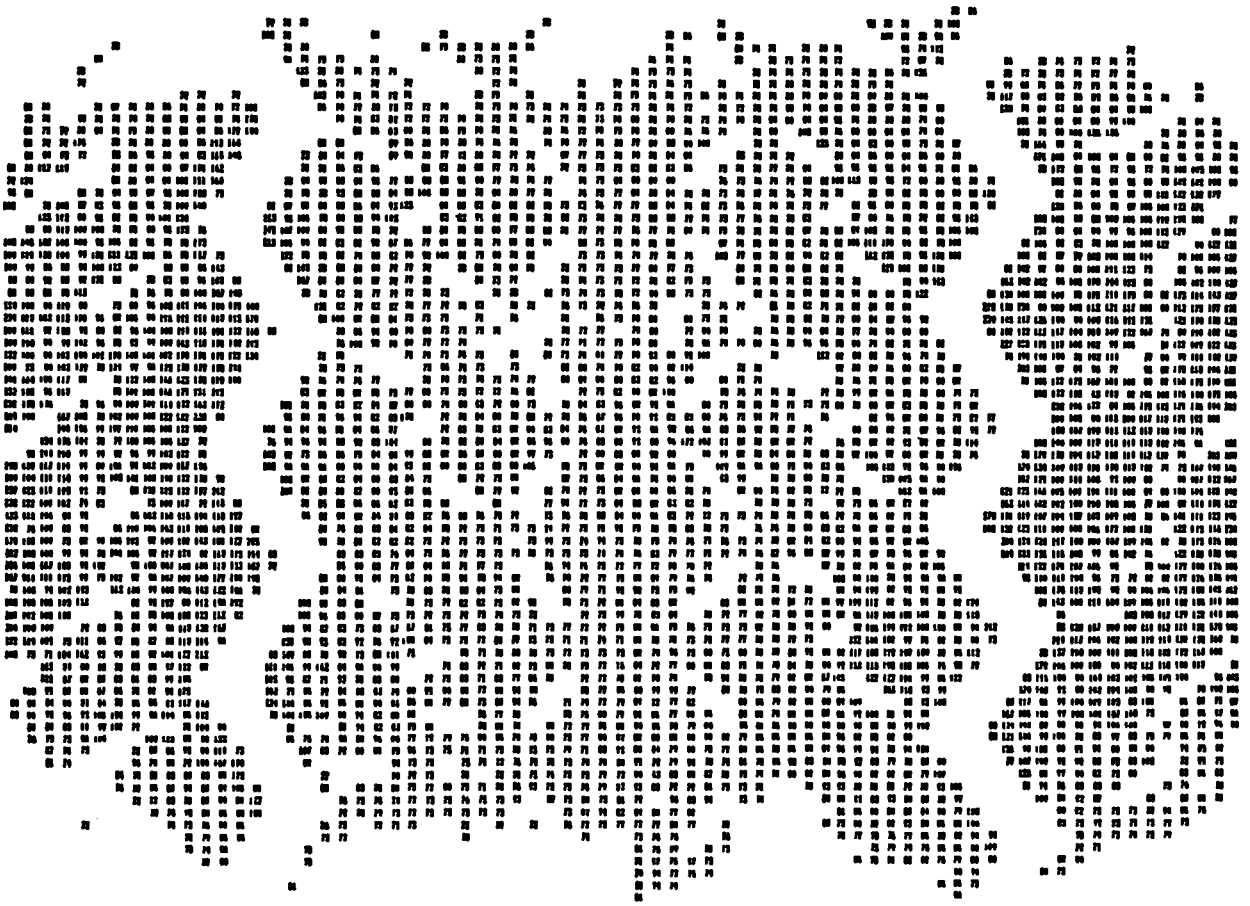

Fig. A.11. Numerical contact pressure print for Tread 9045

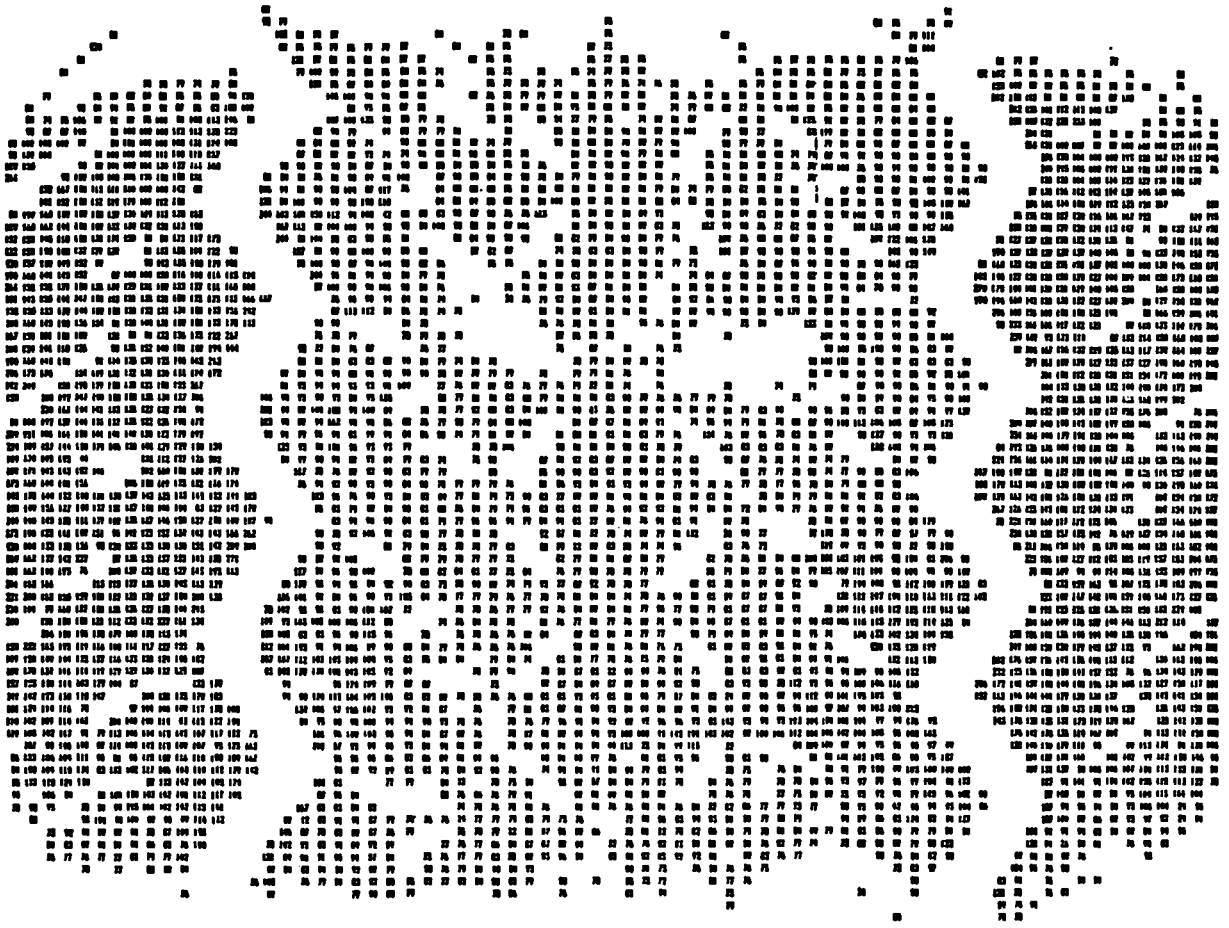

Fig. A.12. Numerical contact pressure print for Tread 9054

APPENDIX B

EXPERIMENTAL DATA FOR MAXIMUM CONTACT PRESSURE, CONTACT AREA AND SUM OF FORCES FOR VARIOUS TREAD TYPES, INFLATION PRESSURES AND AXLE LOADS

TABLE B.1: EXPERIMENTAL DATA FOR MAXIMUM CONTACT PRESSURE, CONTACT AREA AND SUM OF FORCES FOR VARIOUS TREAD TYPES, INFLATION PRESSURES AND AXLE LOADS

TIRE (10 x 20)	INFLATION PRESSURE psi	ACTUAL LOAD lbf	MEASURED SUM OF FORCES	PERCENT DIF.	CORRECTED* SUM OF FORCES	PERCENT DIF.	MEASURED** CONTRACT AREA in^2	MAXIMUM CONTACT PRESSURE	CENTER CONTACT PRESSURE
1) BALD	75	4500	5102	13.4	4773	6.1	61.8	260	124
2) BALD	110	4500	4492	0.2	4122	8.4	53.3	197	197
3) TREADED	75	4500	4677	3.9	4176	7.2	51.3	240	93
4) TREADED	90	4500	4608	2.4	4177	7.2	49.0	245	96
5) TREADED	90	5400	6005	11.2	5184	4.0	53.6	306	88
6) TREADED	110	4500	5057	12.4	4398	2.3	48.7	265	121

* Sum of forces corrected for relative humidity and temperature.

** Contact area measured using special program (Validator)

Note: Percent differences are for adjacent measured sum of forces relative to actual applied load.